

The Effects of the COVID-19 Lockdowns on the Composition of the Troposphere as Seen by IAGOS at Frankfurt.

Hannah Clark¹, Yasmine Bennouna^{2,4}, Maria Tsivlidou², Paweł Wolff², Bastien Sauvage², Brice Barret², Eric Le Flochmoën², Romain Blot², Damien Boulanger⁵, Jean-Marc Cousin², Philippe Nédélec², Andreas Petzold³, and Valérie Thouret²

¹IAGOS-AISBL, 98 Rue du Trône, Brussels, Belgium

²Laboratoire d'Aérologie (LAERO), CNRS and Université de Toulouse III, Paul Sabatier, Toulouse, France

³Forschungszentrum Julich, Institute of Energy and Climate Research 8: Troposphere, Jülich, Germany

⁴Royal Netherlands Meteorological Institute (KNMI), De Bilt, the Netherlands

⁵Observatoire Midi-Pyrénées (OMP-SEDOO), CNRS and Université de Toulouse III, Paul Sabatier, Toulouse, France

Correspondence: Hannah Clark (hannah.clark@iagos.org)

Abstract. The European Research Infrastructure IAGOS (In-service Aircraft for a Global Observing System) equips commercial aircraft with a system for measuring atmospheric composition. A range of essential climate variables and air quality parameters are measured throughout the flight, from take-off to landing, giving high resolution information in the vertical in the vicinity of international airports, and in the upper-troposphere/lower-stratosphere during the cruise phase of the flight.

5 Six airlines are currently involved in the programme, achieving a quasi-global coverage under normal circumstances. During the COVID-19 crisis, many airlines were forced to ground their fleets due to a fall in passenger numbers and imposed travel restrictions. Deutsche Lufthansa, a partner in IAGOS since 1994 was able to operate a IAGOS-equipped aircraft during the COVID-19 lockdown, providing regular measurements of ozone and carbon monoxide at Frankfurt airport. The data form a snapshot of an unprecedented time in the 27 year time-series. In May 2020, we see a 3932% increase in ozone near the
10 surface with respect to the 26 year climatologya recent reference period, a magnitude similar to that of the 2003 heatwave. The anomaly in May is driven by an increase in ozone at nighttime which might be linked to the reduction of NO during the COVID-19 lockdowns. The anomaly diminishes with altitude becoming a slightly negative anomaly in the free troposphere. The ozone precursor carbon monoxide shows an 11% reduction in MAM near the surface. There is only a small reduction of CO in the free troposphere due to the impact of long-range transport on the CO from emissions in regions outside Europe. This
15 is confirmed by IASI-SOFRID CO retrievals which display a clear drop of CO at 800 hPa over Europe in March but otherwise show little change to the abundance of CO in the free troposphere.

Copyright statement. TEXT

1 Introduction

The World Health Organization declared the global COVID-19 pandemic in March 2020 (WHO, 2020). The serious threat to 20 public health led countries to adopt lockdowns and other coordinated restrictive measures aimed at slowing the spread of the virus. Such measures had an important effect on economic activity and by consequence on the emissions of primary pollutants from industrial and transport sectors. Much discussed, is the extent to which these lockdowns have had a significant effect on local air quality and more widely on atmospheric composition (e.g. Bauwens et al. (2020), Lee et al. (2020)) and climate (Le Quéré et al., 2020).

25 Many studies have focused on primary pollutants such as NO₂, decreases of which were almost immediately apparent in satellite imagery from the TROPOspheric Monitoring Instrument (TROPOMI) on the Sentinel-5 Precursor satellite (Veefkind et al., 2012) over China in January/February (Liu et al., 2020), and later over Europe (Bauwens et al., 2020). Emissions of NO₂ are strongly linked to economic activity

citepDuncan2016. Instruments such as TROPOMI have registered weekly cycles of NO₂ and drops in NO₂ related to behaviour patterns of work and holiday periods (Beirle et al., 2003; Tan et al., 2009). Thus, the large reductions in NO₂ in the 30 tropospheric column during lockdown over the most economically active areas of Europe (in particular the Po valley, Italy) were quickly associated with the drop in industrial output and emissions from transport. Reductions of between 20 and 38% compared with the same periods in previous years were recorded (Bauwens et al., 2020). However, TROPOMI is a young instrument, launched in October 2017, and as such, there is not a robust climatology with which to compare these changes during 35 lockdown, and in particular to control for the influence of different meteorological conditions (e.g. Goldberg et al. (2020)). Relevant weather conditions might include higher planetary boundary layer heights which drive down the surface concentrations of pollutants irrespective of any changes in emissions; windy periods, with their impact on the dispersion and deposition of NO₂; and cloudy skies with their impact on satellite retrievals. As TROPOMI is sensitive to clouds, using only cloud-free columns can lead to a negative sampling bias. In many parts of Europe, skies were unusually clear (van Heerwaarden 40 et al. (2021); (<https://surfobs.climate.copernicus.eu/stateoftheclimate/march2020.php>) due to the persistence of anticyclonic conditions and strongly reduced air traffic (Schumann et al., 2021b, a), and a negative bias may have been reinforced during the lockdown period (e.g. Barré et al. (2021); Schiermeier (2020); <https://atmosphere.copernicus.eu/flawed-estimates-effects-lockdown-measures-air-quality-derived-satellite-observations>).

Drops in primary pollutants were also evident from ground-based air-quality networks across Chinese and European cities; 45 see the review by Gkatzelis et al. (2021) for a comprehensive overview. In Spain's two largest cities, where lockdowns were extremely strict, the reductions of NO₂ concentrations were 62% and 50% (Baldasano, 2020). Lee et al. (2020) calculated an average reduction of NO₂ of 42% across 126 sites in the UK, with a 48% reduction at sites close to the roadside due to the drop in traffic emissions. Wang et al. (2020b) looked at six different pollutants (PM2.5, PM10, CO, SO₂, NO₂, and O₃) and found large reductions in NO₂ from traffic sources and a smaller reduction in CO from reduced industrial activities in Northern 50 China. Similarly, Shi and Brasseur (2020) also noted a drop in CO across the monitoring stations in Northern China operated by the China National Environmental Monitoring Center. Pathakoti et al. (2021), looked at CO from TROPOMI compared with

the climatology from the MOPITT (Measurements of Pollution in the Troposphere) satellite and noted that the CO levels were lower during the first phase of the lockdown over India but higher during the second phase. This was probably indicative of the longer lifetime of CO in the atmosphere, and the long- range transport of CO from a variety of global sources. Overall, the 55 reductions in NO₂ and CO in near-surface air masses due to COVID-19 lockdown conditions range from 20% to 80% for NO₂ and 20% to 50% for CO, for all observations reported globally (Gkatzelis et al., 2021).

The effects on the secondary pollutant ozone, are more complex due to its chemistry. Tropospheric ozone is produced by photochemical oxidation of methane, carbon monoxide, and non-methane volatile organic compounds (NMVOCs) in the presence of nitrogen oxides (NO_x=NO + NO₂). There is also a contribution from stratosphere-to-troposphere transport (Holton et al., 1995) in certain synoptic situations (Stohl et al., 2005; Gettelman et al., 2011; Akrutidis et al., 2018). Near the surface, ozone is lost through dry deposition, titration by NO and reactions with hydrogen oxide radicals (HO_x) (Monks, 2005). The fall in ozone precursors such as CO during lockdown, together with a decrease in available quantities of the NO_x catalyst, might have been expected to lead to a fall in ozone. However, Wang et al. (2020b) found that over China, O₃ increased, possibly because a lower atmospheric loading of fine particles led to less scavenging of HO₂, and greater O₃ production as a result. 60 Such effects have been noted over China during the summers of 2005-2016 (Wang et al., 2020a) and so are not unique to the lockdown period. Shi and Brasseur (2020) also found that ozone increased by a factor of two over northern China specifically noting the wintertime conditions during lockdown. Over southern Europe, ozone was also seen to increase up to 27% in some places, explained by the reduction in NO_x and lower titration by NO (Sicard et al., 2020). Ordóñez et al. (2020) cautioned that whilst NO₂ fell across the whole European continent, the ozone anomalies were not always of the same sign. Ozone decreased 65 over Spain but increased over much of Northwest Europe where meteorological conditions were favorable for ozone formation, including elevated temperatures, low specific humidity and enhanced solar radiation.

A similar picture is drawn from the collection of data from world-wide near-surface observations as reported by Gkatzelis et al. (2021). The fractional changes for ozone range from a decrease by 20% in Central Asia (4 studies) to an increase of up to 20% for several parts of the world (Africa: 2 studies; South America: 17 studies; West Asia: 17 studies; Southeast Asia: 19 70 studies). For Europe (134 studies), percentage changes in ozone are on average close to zero with few reported reductions of less than 20% and increases of up to 65%. Although most of the reported data sets include the consideration of meteorological conditions, this variability highlights the dominant role of the meteorological situation in creating these ozone anomalies at the surface.

Fewer discussions have considered the free troposphere where measurements would be indicative of global or background 80 changes in the levels of pollutants. Steinbrecht et al. (2021) looked at free tropospheric ozone across the northern hemisphere from ~~balloon and sonde~~ balloon-borne ozonesonde measurements from 1-8km in altitude. They found a reduction in free tropospheric ozone of about 7% compared with the 2000-2020 climatological mean which they largely attributed to the reduction in ~~pollution~~ emissions during the COVID-19 lockdowns.

The IAGOS (In-service Aircraft for a Global Observing System) instruments carried on commercial aircraft measure the 85 primary pollutant carbon monoxide and the secondary pollutant ozone, along with water vapour, clouds and meteorological parameters such as temperature and winds (Petzold et al., 2015; Nédélec et al., 2015). Ninety percent of the data are acquired

in the upper troposphere-lower stratosphere (UTLS) when the aircraft attain cruise altitude somewhere between 300 and 180 hPa (9 to 12 km above mean sea level). The remaining 10% of data are collected during landing and take-off over more than 300 airports around the world. During the COVID-19 lockdowns in Europe, there was a large fall in passenger numbers with a 90 consequent impact on the number of IAGOS aircraft flying, and the amount of data collected. However, one of the Lufthansa aircraft was converted to carry cargo, and operated throughout the lockdown period. The aircraft made regular flights from Frankfurt to Asia carrying important medical supplies. Frankfurt airport has the longest, densest and most homogeneous time-series of all the airports visited by IAGOS. Thus, the climatology calculated there is the most robust (Petetin et al., 2016b) with ozone being measured since 1994 and CO since the end of 2001.

95 In this article, we present the observed anomalies of both ozone and CO seen over Frankfurt and benefit from the fine 30m vertical resolution throughout the troposphere, to distinguish the surface anomalies from the observations in the free troposphere. This offers a valuable check on satellite data, and adds unique and valuable vertical information which is not offered by surface sites. We judge the significance of the ozone anomalies against the 26 year climatology (1994-2019) at Frankfurt, putting the observed anomalies in context with other important events such as the heatwave in 2003. To complement 100 the IAGOS data at Frankfurt we use IASI-SOFRID CO retrieval which give an idea of the extent of any regional changes over Europe.

2 Data

The research infrastructure IAGOS, is described in detail in (Petzold et al., 2015). Using commercial aircraft as a platform, IAGOS instruments make routine measurements of ozone, and carbon monoxide along with water vapour, cloud particles and 105 meteorological parameters including temperature and winds. A full description of the instruments that measure ozone and CO used here, can be found in (Nédélec et al., 2015). The ozone instrument, a dual-beam ultraviolet absorption monitor has a response time of 4 s, and an accuracy estimated at about 2 ppbv (Thouret et al., 1998). This 4 second response time corresponds to a vertical distance of about 30 m. In the horizontal, the aircraft covers a distance of about 80km during the first 5km of ascent (Petetin et al., 2018a). Therefore during the ascent and descent phases of the flight, IAGOS provides fine-scale quasi-vertical 110 profiles. Carbon monoxide is measured with an infrared analyser with a time resolution of 30 s (7.5 km at cruise speed of 900 km h⁻¹) and a precision estimated at 5 ppbv (Nédélec et al., 2003)

IAGOS began life in 1994 under the name MOZAIC (Measurement of Ozone and Water Vapour on Airbus in-service Aircraft) (Marenco et al., 1998) and as such IAGOS has provided a long time-series of ozone data over 27 (1994-present) years, and of CO for almost 20 years (2001-present). The homogeneity of the time-series since 1994 has been demonstrated 115 by (Blot et al., 2021), giving confidence that IAGOS data can be used for a robust climatology and for the study of long-term trends. As mentioned above, this gives IAGOS some important advantages over more short-lived data-sets such as those from satellites, and allows us to put any anomalies into context within the same reference observations.

For the IAGOS measurements, a number of auxiliary, diagnostic fields are delivered with the data as standard level 4 products. These include potential vorticity, geopotential height and boundary layer height which we will use in this article. The

120 boundary layer height which is defined as the boundary layer thickness (zPBL) + orography is calculated by interpolating the European Centre for Medium-Range Weather Forecast's (ECMWF) operational boundary layer heights to the position and time of the IAGOS aircraft. The ECMWF fields were 1° horizontal resolution and 3 hour time resolution with 60, 90 or 137 levels in the vertical depending on the time period used ([http://www.iagos-data.fr/#L4Place:\)](http://www.iagos-data.fr/#L4Place:).

125 In order to determine the ~~geographic~~ geographical origin and source of the CO measured by IAGOS, a tool known as SOFT-IO (Sauvage et al., 2017a, b) has been developed, that uses FLEXPART (Stohl et al., 2005; Forster et al., 2007) to link the IAGOS measurements with emissions databases via 20-day back trajectories. For the entire IAGOS flight track, SOFT-IO v1.0 (Sauvage et al., 2017a, 2018) estimates the source region of the CO contribution from 14 different world regions of emissions from the Copernicus Global Fire Assimilation System GFAS v1.2. The source regions are as defined by the Global Fire Emissions Database (GFED), although the emissions inventories are GFAS. It can also estimate the contributions 130 from anthropogenic sources or wildfires. As for the auxiliary diagnostic fields mentioned above, the meteorological data for FLEXPART come from the 1° by 1° ECMWF operational analyses and forecasts with a 6 hour and 3 hour time resolution respectively (Sauvage et al., 2017b).

135 To set the IAGOS measurements at Frankfurt airport into a regional context, we use CO satellite retrievals from the Infrared Atmospheric Sounding Interferometer (IASI) on the MetOp meteorological platforms (Clerbaux et al., 2009). These retrievals are performed with the SOftware for a Fast Retrieval of IASI Data (SOFRID) described in Barret et al. (2011); De Wachter et al. (2012). This software is based on the RTTOV (Radiative Transfer for TIROS Operational Vertical Sounder) operational radiative transfer code (Saunders et al., 1999; Matricardi et al., 2004) combined with the 1D-Var software (Pavelin et al., 2008). For CO₂ the SOFRID retrievals provide a maximum of two pieces of information about the vertical profiles from the surface to the lower stratosphere with a maximum sensitivity at about 800 hPa and an estimated error of about 10 % (De Wachter et al., 140 2012).

2.1 Anomalies of ozone in early 2020

In this first section, we look at the anomalies of ozone which were strongly evident in spring 2020. Figure 1, shows the ~~seasonally~~ averaged profile of ozone measured at Frankfurt for ~~March–April–May~~ March and May 2020. ~~There were no ozone data in April 2020, due to the ozone sensor being inoperative.~~ The data were acquired by one of the IAGOS-equipped Lufthansa 145 passenger aircraft which was based at Frankfurt. It was converted to cargo operations and was kept flying throughout the lockdown period making a total of 84 flights ~~from March–May~~ in March and May 2020.

In Fig. 1, the IAGOS observations are marked by the black solid line. The blue solid line represents the ~~seasonal~~ average for the ~~26 year (1994–2019) reference climatology, reference time-series 2016–2019~~ and the blue shaded envelope shows the inter-annual variability of ~~MAM~~ March&May over this period. ~~Similar averaged profiles were presented in (Petetin et al., 2016b) We used a short and recent section of the timeseries of ozone to account for any recent changes in background amounts of ozone. Petetin et al. (2016b) found only a weakly significant trend in ozone at Frankfurt in the lower troposphere over the period 1994–2012. Gaudel et al. (2020) considered the free troposphere from 700 to 250 hPa and the period 1994–2016 and found small increases in ozone over Europe, and Cooper et al. (2020) found increases in the free troposphere over Europe~~ based 150

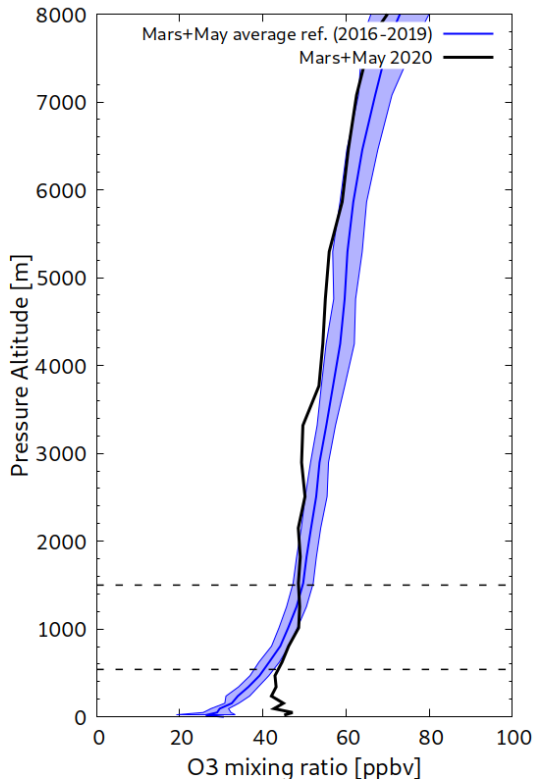


Figure 1. IAGOS observations of ozone for ~~March-April-May (MAM)~~ 2020 in black. The blue line is the average profile for ~~MAM~~ ~~March&May~~ calculated over the ~~reference~~ time-series (220 profiles) of the ozone observations ~~(1994-2019)~~ ~~2016-2019~~. The shaded area represents ± 1 standard deviation of the ~~season MAM~~ interannual variability for ~~March& May~~ over ~~this the~~ reference period ~~i. e.~~ ~~Horizontal~~ lines denote the ~~interannual variability~~ boundaries of the ~~MAM season~~ sections of study as used in subsequent figures.

on the ~~period 1994-2012. The climatological profiles presented here and in Petetin et al. years 1994-2017. Because of the~~ considerable variability in the magnitude of trends over time, altitude and season, we compare our results to a recent reference 155 period 2016-2019.

The profiles presented in Fig. 1 are similar to those presented in (Petetin et al., 2016b) based on the period 1994-2012. They show the maximum ozone mixing ratios in the free troposphere to be about 60 ppbv increasing from 21 ppbv at the ground and which then increase again in the upper troposphere. In the period MAM 2020, there were notable departures from the 160 climatology. Ozone mixing ratios reached on average 42 ppbv in a layer from the surface up to an altitude of 1000m. Such values are more commonly found during summer heatwaves. In the free troposphere from 2000-5000m, the abundance of ozone is lower than normal, lying outside the expected interannual range. We consider some possible reasons for these anomalies ~~in the~~, ~~in particular the possible link with the COVID-19 lockdowns, in the~~ following sections.

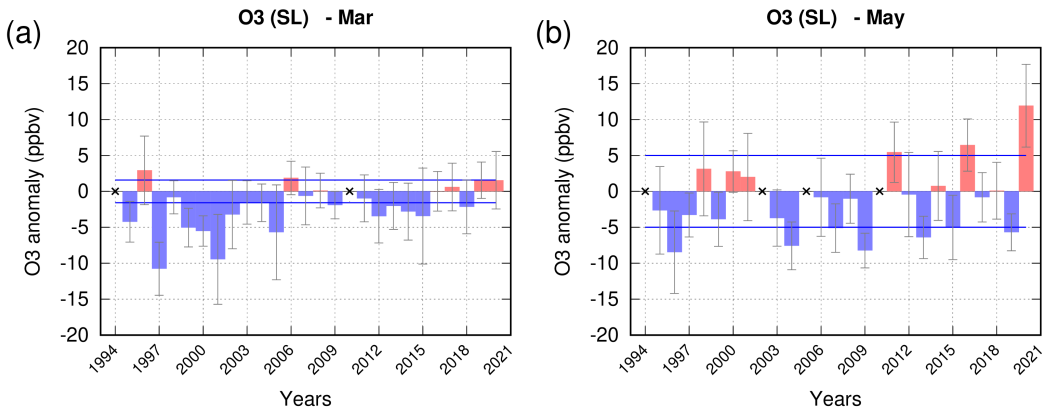


Figure 2. Anomalies of ozone for 1994-2020 calculated with respect to 2016-2019 for all the months of (a) March, (b) May for the surface layer ($>950\text{hPa}$). There were no ozone data in April 2020. The grey bars represent the 95% confidence limits, and the blue horizontal lines represent the interannual variability.

2.1.1 Anomalies of ozone in the surface layer ($>950\text{hPa}$)

165 The period MAM 2020 corresponded to the period with the most stringent COVID-19 lockdowns across western Europe, but each country had its own date of onset, duration, and ~~different levels~~ ~~level~~ of severity. Measures of European mobility (Grange et al. (2021), based on Google mobility data) reveal that the depths of lockdown were in early April, showing a very slight recovery throughout May. At Frankfurt airport, there was 50% less ~~traffic~~ ~~air-traffic~~ in March 2020 compared with March 2019, with nearly 80% less ~~traffic~~ ~~air-traffic~~ in April and May (source, FRAPORT <https://www.fraport.com/en/investors/traffic-figures.html>, last accessed 18 December 2020). ~~This reduction was driven by a fall in passenger numbers as lockdown measures increased around the world.~~ According to Grange et al. (2021), the restriction measures began in Germany on 22nd March 2020 and had a “~~Stringency~~ ~~stringency~~ index” defined as “a measure of the strictness of ‘lockdown style’ policies”, that remained relatively high until the end of May, but ~~that the lockdown~~ was by no means the strictest in Europe. ~~Anomalies of ozone for 1994-2020 for all the months of (a) March, (b) May for the surface layer ($>950\text{hPa}$). There were no ozone data in April 2020.~~

170 175 In Fig. 2, we present the anomalies in ozone for the individual months of March and May 2020. ~~We~~ As mentioned above, ~~we~~ did not have any ozone data in April 2020. ~~We require there to be 7 days to make the monthly average otherwise the month is excluded. Excluded months are marked with a cross. During the lockdown period, there were fewer flights than normal and we need to be aware of any sampling bias that this may introduce. The number of profiles per month is shown as the solid grey bars in top panel of figure 3. The confidence limits, shown in Fig. 2, account for the differing number of profiles per month.~~ The confidence limits are calculated using a Student’s t-distribution.

180 It was during the month of May, after the lockdown had been in place for several weeks, when the ozone anomaly in the surface layer (pressure $P > 950\text{hPa}$) was most pronounced (Fig. 2). ~~We require there to be 7 days to make the monthly average otherwise the month is excluded. Excluded months are marked with a cross.~~ In May, ozone was recorded at 13.9 ppbv

(~~39~~+11.9ppbv (+32%) higher than the reference average (~~1994-2019~~~~2016-2019~~) and was the largest anomaly for the month
185 of May since the time-series began in 1994. The ~~anomaly~~ magnitude of the anomaly including the 95% confidence limits are
outside the interannual variability, based on the reference years, given by the solid blue line. The ~~anomaly~~ is apparent in the
first ~~800m~~-1000m of the atmosphere (Fig. 1). A positive anomaly was also observed in March 2020 (~~155%~~) with a smaller
value compared with May. Positive anomalies in ozone have not been unusual in recent years (see Fig. 3) suggesting that the
lockdowns are not the only explanation.

190 To set the magnitude of these anomalies into context with other periods, the time-series for each month for the surface layer
over Frankfurt, is shown in the ~~top-bottom~~ panel of Fig. 3. ~~In addition to the monthly averages, we also show the number of
profiles per month as the solid grey bars. During the lockdown period, there were fewer flights than normal and we need to be
aware of any sampling bias that this may introduce. The bottom panel of the plot shows a time-series of the monthly anomalies
in the surface layer from 1994-2020~~
195 ~~The anomalies are calculated with respect to 2016-2019. There were a number of few~~
occasions when the ozone anomalies were comparable to that of May ~~2020. These 2020 including a peak of similar magnitude
in February 2005. In the other seasons, the peaks~~
were August 2015 and September 2016 when there were short heatwaves, and the ~~other was the~~ well known heatwave in August 2003 which we discuss here as it was well documented with IAGOS data
(Tressol et al., 2008; Ordóñez et al., 2010). ~~It should be noted that, when compared with the recent reference period 2016-2019,
the magnitude of the anomaly in August 2003 is diminished, suggesting that these high ozone abundances have become less
unusual.~~
200

An increase of ozone near the surface can result from increased production of ozone, or reduced sinks of ozone, depending
on the conditions and the time of day. Positive anomalies of ozone may be due to an increase in the precursors of ozone,
or a prevalence of certain meteorological conditions including increased UV radiation, stagnant airmasses or lower boundary
layer heights which trap the pollutants near the surface. Otherwise, there can be a decrease in the sinks of ozone, such as a
205 decrease in the rate of dry deposition or a decrease in titration by NO due to a reduction in the ~~reservoir of NO~~emissions of
~~NOx~~. During the 2003 heatwave, IAGOS data showed that there were positive anomalies at Frankfurt in both ozone and the
precursor carbon monoxide in the low troposphere, with the ozone anomalies up to 2.5km deep and with the magnitude of the
anomalies increasing towards the surface (Tressol et al., 2008). Tressol et al. (2008) found that near the surface, ozone was
almost twice the normal amount, and CO was more than 20% higher. The increased CO was due to the transport of plumes
210 from wildfires over Portugal exacerbated by the dry conditions created by the heatwave. Thus, during the 2003 heatwave, the
increased ozone was caused by an increase in precursors and the favorable meteorological conditions.

During lockdown, the chemical environment was quite different. The positive ~~ozone anomaly~~ anomaly of ozone was
accompanied by a drop in the amount of NO as evidenced by the TROPOMI satellite ~~measurements of~~ NO₂ (Bauwens
et al., 2020), and there is some evidence from IAGOS measurements that levels of the precursor carbon monoxide also
215 fell (see section 2.2). The ~~ozone anomaly~~ anomaly of ozone in the surface layer (~~extending to 1km c.f. 2.5km in the 2003
heatwave~~) was most likely due to the combination of increased ~~ozone production~~ production of ozone due to the exceptionally
sunny conditions across a large sector of northern Europe (van Heerwaarden et al. (2021); Ordóñez et al. (2020) , see also
<https://surfobs.climate.copernicus.eu/stateoftheclimate/may2020.php>) along with the removal of one of the ozone

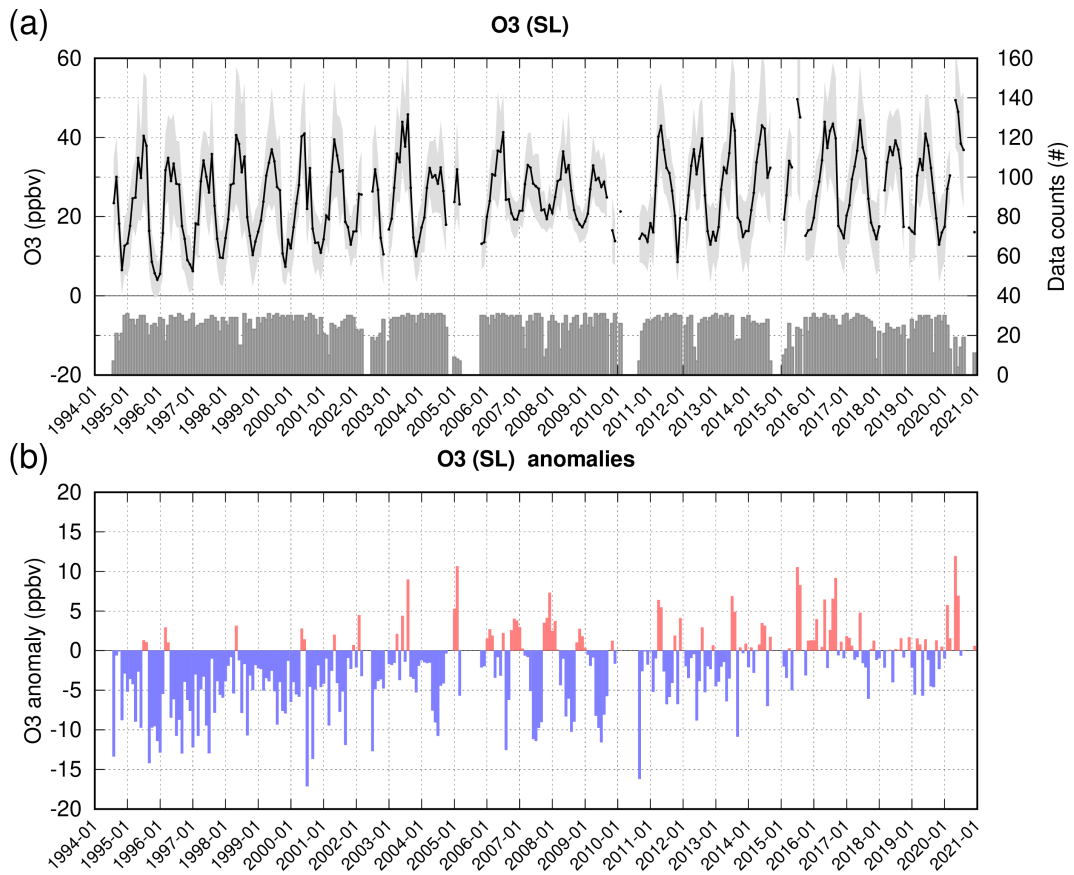


Figure 3. Monthly time-series for 1994-2020 of O₃ for the surface layer over Frankfurt (a). The grey bars represent the number of daily profiles used to calculate the monthly means shown in black. Grey shading represents the standard deviation of the monthly mean values for each month. (b) The monthly anomalies calculated with respect to the reference average 1994-2019-2016-2019 in the surface layer.

sinks, particularly the reduction in ozone titration because of the reduction in NO. In addition, the stable meteorological conditions, lack of wind, and air stagnating over towns, could also have contributed to the accumulation of pollutants and of ozone itself in the boundary layer. Some recent studies have attempted to tease out the contribution of meteorology from the impact of the changes in the emissions of precursors (Ordóñez et al., 2020; Petetin et al., 2020; Lee et al., 2020). All found that there were important and differing impacts of meteorology, but that the photochemical effects from NO_x were dominant there were changes in NO_x that were unattributed to the meteorological conditions and linked to falling emissions during the lockdowns.

The magnitude of any anomaly may be significantly influenced by the sampling times within the diurnal cycle. Petetin et al. (2016a), described the typical diurnal cycle of ozone at Frankfurt airport observed with IAGOS data at different altitudes. They noted that the mixing ratios of ozone are minimum at nighttime due to dry deposition and titration by NO in the shallow nocturnal boundary layer and reach a maximum in the afternoon, due to photochemistry and mixing with ozone-rich layers above the boundary layer. Petetin et al. (2016a) showed the diurnal cycle of ozone at Frankfurt to be maximum between 12:00

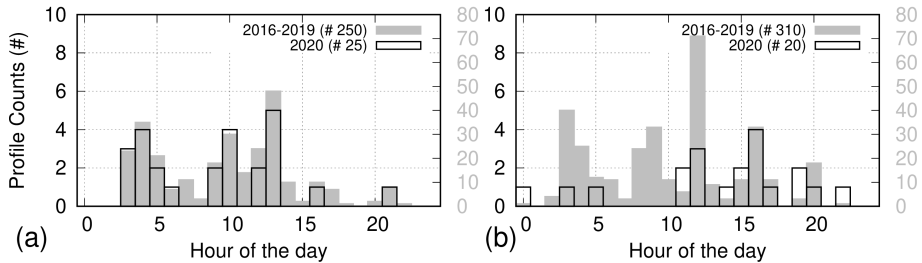


Figure 4. Number of profiles by hour of the day (UTC) for a)March 2020 and b)May 2020 (counts on left-hand axis) compared with May over the same months in the reference period 1994-2019/2016-2019 (counts on right-hand axis).

230 and 18:00 UTC in MAM in the layers below 900hPa. The amplitude is maximum at the surface and decreases with altitude, becoming almost insignificant at altitudes above 900hPa. We consider the anomaly observed in May with respect to the diurnal cycle of ozone. More measurements in the afternoon would lead to an oversampling of the maximum and a positive ozone anomaly, and conversely, more measurements at nighttime would be an oversampling of the minimum and a negative anomaly. In Fig. 4, we can see the hourly distribution of the IAGOS profiles for the month of months of March and May in 2020 235 compared with the same month for months in the reference period 1994-2019/2016-2019. In the climatology, there is a bias towards early morning measurements and in measurements in early morning. In March 2020, the distribution is similar to the that during the reference period, but in May 2020 there is a bias towards measurements in early afternoon. This reflects the different flight operations carried out during the COVID-19 period.

To account for this bias, we calculate the anomaly for May for the daytime hours when the diurnal cycle is maximum (10:00- 240 18:59 UTC) and the nighttime hours when the diurnal cycle is minimum (00:00-09:00 & 19:00-23:59 UTC) applying this to both the climatology and 2020. These are shown in 2020 (Fig. 5(a) and (b) respectively). This is based on the diurnal cycle for ozone at Frankfurt in MAM described in Petetin et al. (2016a) and depends upon ozone photochemistry and the dynamical development of the boundary layer. In Fig. 5 (a) there is still remains a significant increase of ozone in May during the day (8.3ppbv, 19%), comparable with other anomalies which have occurred 4 times during the last 26 years. This likely reflects the 245 meteorological conditions that were relatively exceptional and favorable to ozone formation. In Fig. 5 (b) the nighttime increase (12.8ppbv, 419.9ppbv, 29%) is clearly the most significant observed in the time-series highlighting the drop in NO₂. We infer that the positive anomaly in ozone at night is linked to the drop in NO₂ at Frankfurt (Barré et al., 2021) during lockdown and the consequent reduction in ozone titration.

Once meteorological changes were accounted for, the estimates of lockdown-induced NO₂ changes for Frankfurt were -24% 250 and -33% based on TROPOMI observations and surface stations respectively (Barré et al., 2021). The positive ozone anomaly observed in IAGOS data for the surface layer is in agreement with the other studies cited based on the surface networks and as reviewed by (Gkatzelis et al., 2021). The IAGOS data for the remainder of 2020 (Fig. 3), show smaller positive anomalies which were not significant within the time-series, suggesting that the anomaly in MAM, was short-lived. We now explore the vertical extent of the ozone anomaly, using the unique perspective that IAGOS offers.

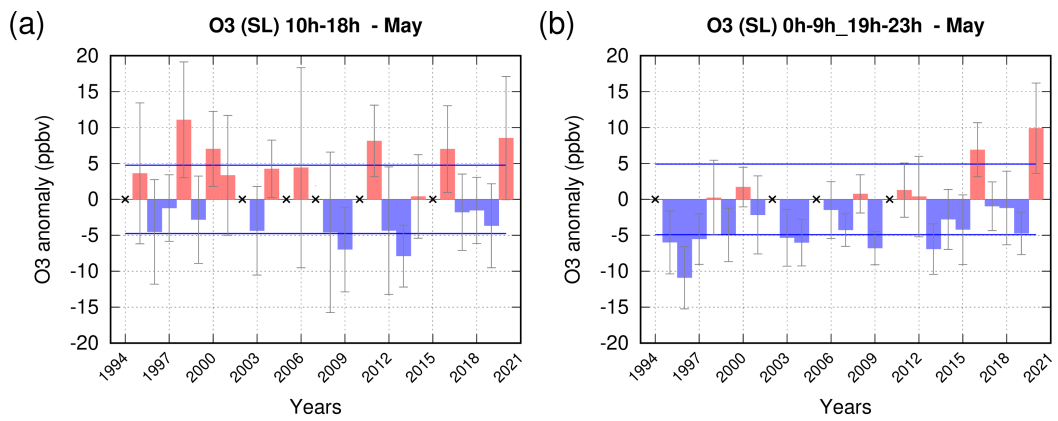


Figure 5. Anomalies of ozone for 1994-2020 for all the months of May in the surface layer (>950hPa) for the a) daytime (10:00-18:59 UTC) and b) nighttime (00:00-09:00 & 19:00-23:59 UTC). The grey bars represent the 95% confidence limits, and the blue horizontal lines represents the interannual variability.

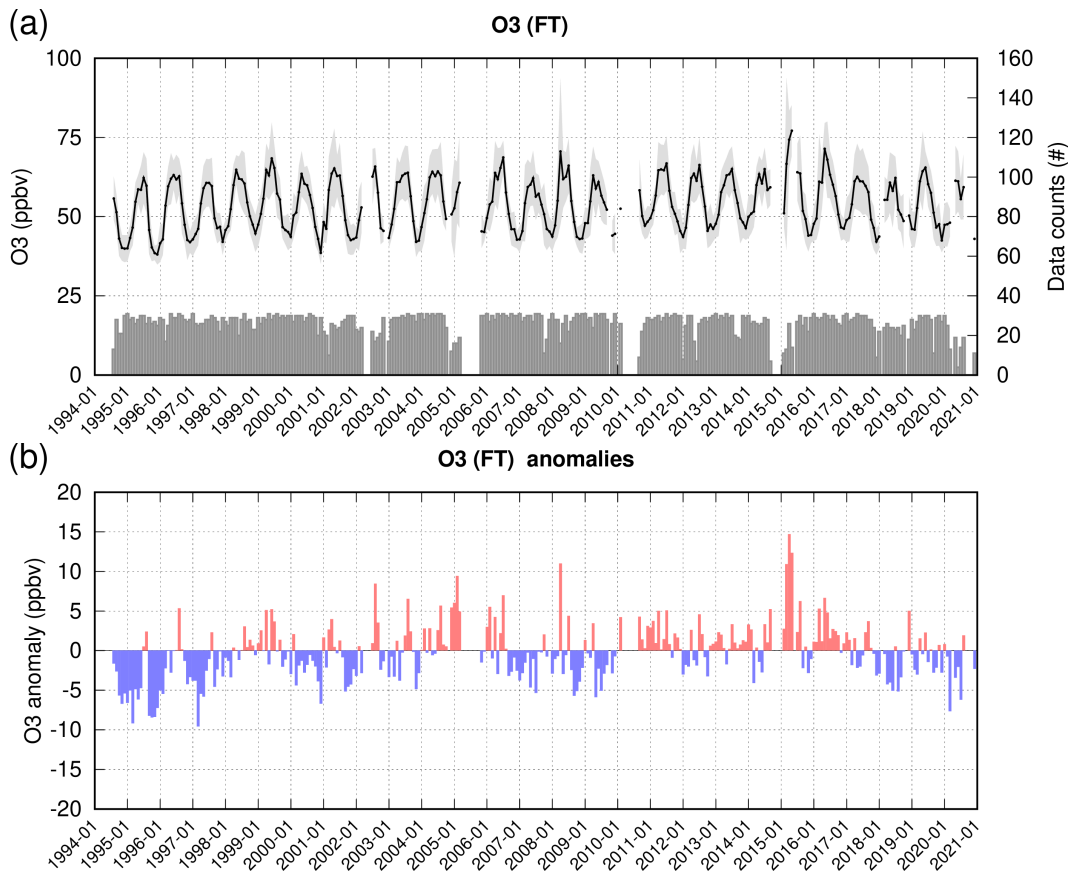


Figure 6. Monthly time-series for 1994-2020 of O₃ for the free troposphere (850-350hPa) over Frankfurt (a). The grey bars represent the number of daily profiles used to calculate the monthly means shown in black. Grey shading represents the standard deviation ~~of the monthly mean values for each month~~ (b) The monthly anomalies calculated with respect to the reference average ~~1994-2019-2016-2019~~ in the free troposphere.

255 2.1.2 Anomalies of ozone in the free troposphere (850-350hPa)

In contrast to the positive anomaly in the surface layer up to ~~800m~~~~1000m~~, the anomaly in the free troposphere above 2000m is negative (Fig. 1) lying just ~~on the edge outside~~ of the range of interannual variability based on the 26 year time-series shown in Fig. 6. The grey bars in the top panel of Fig. 6 represent the number of available daily profiles in each month (where there were more than 7 days available in the month). There was a ~~-6.7 ppbv or -12% drop~~~~-7.6 ppbv or -14% change~~ in ozone in 260 March (Fig. 7). This negative anomaly is the largest for March since 1997 for the IAGOS observations in the free troposphere. It is too early to have resulted from the European lockdowns, and not easy to link ~~with to~~ the Asian lockdowns. There was only a ~~2.0 ppbv (3%) reduction~~~~-3.4 ppbv (-5%) change~~ in ozone in the free troposphere over Frankfurt in May 2020 which might be linked to regional European lockdowns (Fig. 7), ~~but is not outside the interannual variability~~. We had no data for April

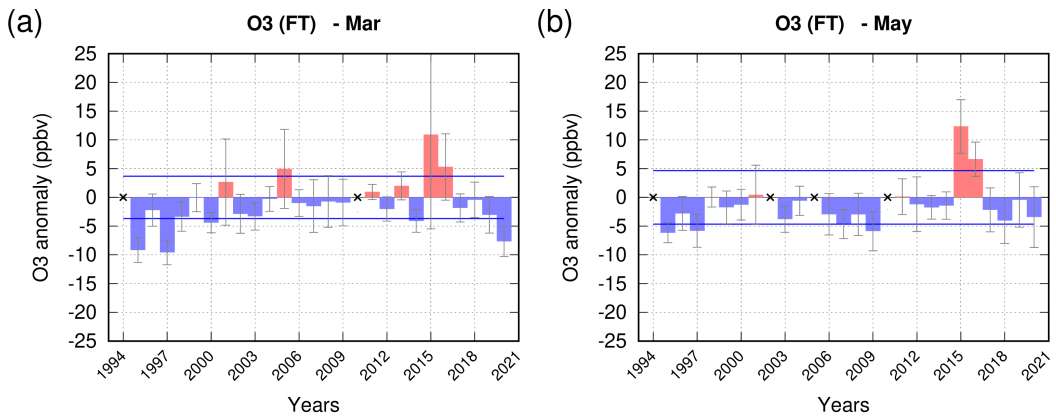


Figure 7. Anomalies of ozone for 1994-2020 for all the months of (a) March, (b) May in the free troposphere (850-350hPa). There were no ozone data in April 2020. [The grey bars represent the 95% confidence limits, and the blue horizontal lines represent the interannual variability.](#)

2020. The IAGOS data show that ozone levels remained lower than usual for several months after the main lockdown period
 265 ended, with an [-11-10%](#) anomaly being observed in July (the largest anomaly recorded for July in the 27 year time-series; see Fig. A1) as the economic recovery and emissions remained suppressed throughout summer 2020 (Fig. 6). Over the period April-August 2020, a 7% drop was seen by [balloons and sondes ozonesondes](#) (Steinbrecht et al., 2021) from 1-8km in altitude. This figure represents a mean value across all sites in the northern hemisphere over the period April-August 2020 compared with the 2000-2020 climatology. The negative anomaly seen at Frankfurt in IAGOS data may illustrate that ozone abundances
 270 fell widely during MAM due to the combined effect of the lockdown measures across Europe, but evidence from the [balloon and sonde data ozonesondes](#) (Steinbrecht et al., 2021) suggests that we can expect a degree of geographical variability. [For example, there was no notable decrease in free tropospheric ozone in the sparsely-sampled Southern Hemisphere.](#)

2.2 Carbon Monoxide in Spring 2020

As mentioned in the introduction, some studies have demonstrated a fall in the ozone precursors during MAM 2020. The 275 reductions in CO in near-surface air masses due to COVID-19 reported by (Gkatzelis et al., 2021) ranged from 20% to 50% for CO. Due to the long (weeks to months) lifetime of CO in the atmosphere, the causes of these decreases in CO are difficult to attribute. Figure 8, shows the seasonally averaged profile of CO measured at Frankfurt for MAM 2020, with the black, solid line denoting the IAGOS observations. The red solid line represents the seasonal average for the reference period 2016-2019, and the red shaded area shows the interannual variability of MAM over the reference period. Often there are fewer IAGOS 280 observations near the surface than in the free troposphere which leads to the standard deviation being greater near the surface as shown by the wider envelope (shaded red area). The ~~inflection~~ inflection of the black curve results from a small number of flights which nevertheless fall within the expected range shown by the red shaded area. Despite the length of the time-series being nearly 20 years, we have chosen ~~a shorter~~ the same ~~short~~ segment (2016-2019) for our reference period ~~as we used~~ for ozone. This is because there is a negative trend in CO (-1.9%yr-1 and 2.0%yr-1 from Petetin et al. (2016b) for lower 285 troposphere and mid-troposphere springtime respectively) and thus all recent data shows a negative anomaly ~~with respect to~~ the period 2001-2019 (see also Fig. 9). We return to this point later. For the period MAM 2020 we can see that the CO mixing ratios are below the average for recent years (red line) and lie at the lower limit given by the envelope of interannual variability.

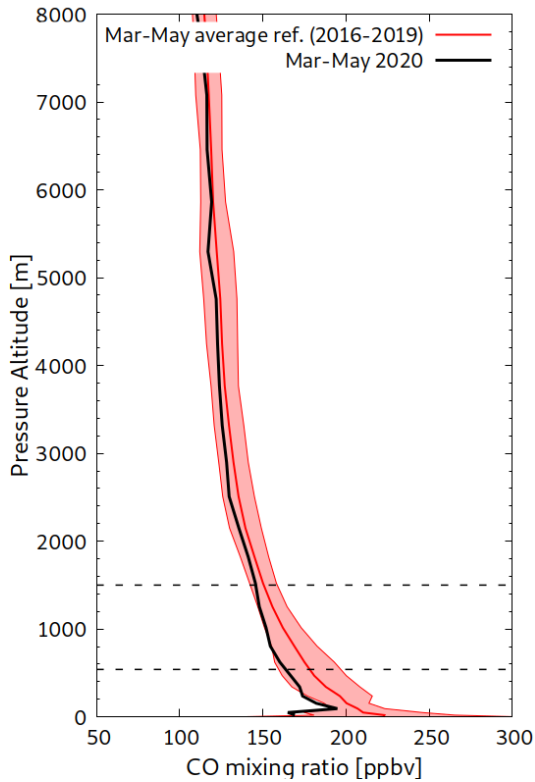


Figure 8. IAGOS observations of CO for March-April- May (MAM) 2020 in black. In red, the average profile for MAM calculated over the reference period 2016-2019 (300 profiles). The shaded area represents ± 1 standard deviation of the seasonal interannual variability for MAM over this reference period. e-Horizontal lines denote the interannual variability boundaries of the MAM seasonsections of study as used in subsequent figures.

Similar averaged profiles were presented in Petetin et al. (2016b) based on the period (2002-2012) where the average mixing ratio at 2000m for MAM was 150ppbv. For our segment 2016-2019 the average mixing ratio for MAM at 2000m was 140ppbv, 290 indicative of the negative trend of CO. Over the period 2002-2020, there has been a drop in CO mixing ratios observed at Frankfurt due to a reduction in emissions and the impact of emissions protocols. However, there is a strong interannual variability in the free tropospheric background which reflects the interannual variability of global biomass burning, anthropogenic emissions, and the complex interactions with other species such as OH and O₃. The background abundance of CO therefore depends on the selected segment of the time-series.

295 **2.2.1 Anomalies of carbon monoxide in the surface layer (>950hPa)**

In the surface layer, we see a downward trend in monthly values of CO on the seasonal and annual scale (see Fig. 9) in agreement with Petetin et al., (2016b). Also shown in Fig. 9, is the number of flights per month as the solid grey bars which

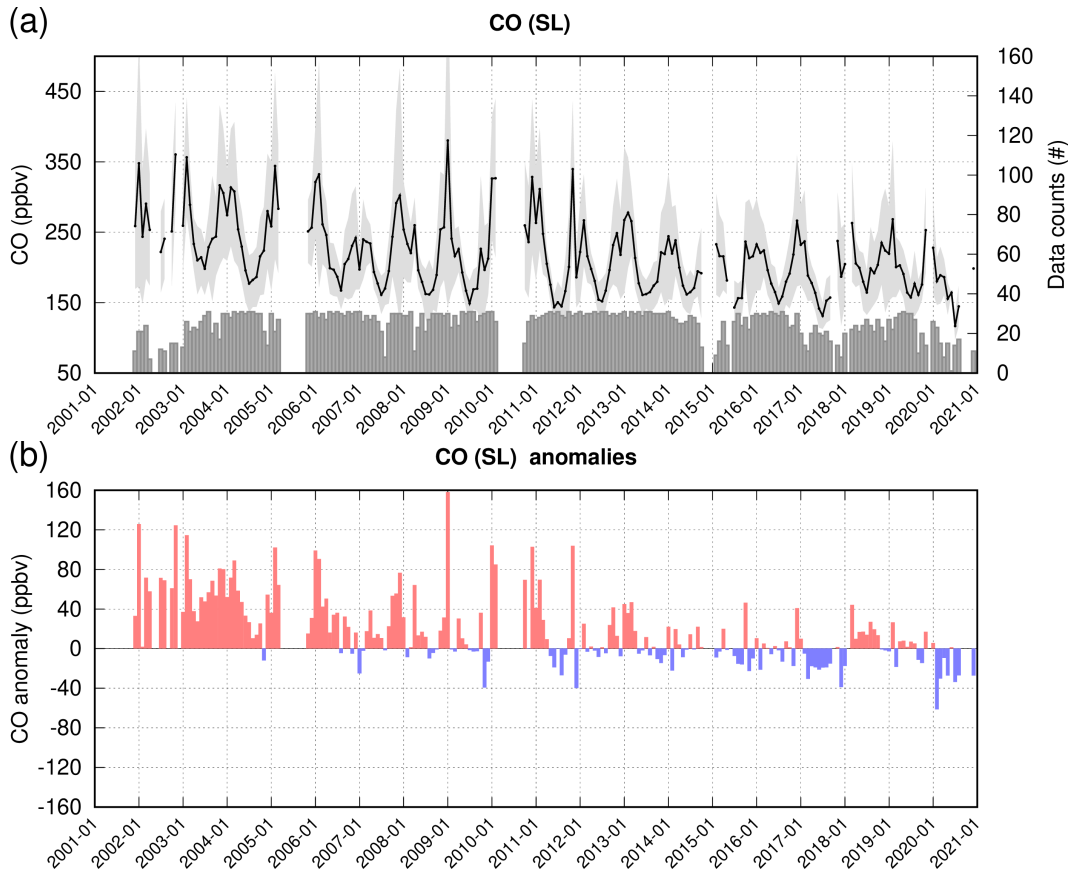


Figure 9. Monthly time-series for 2001-2020 of CO for the surface layer over Frankfurt (a). The grey bars represent the number of daily profiles used to calculate the monthly means shown in black. Grey shading represents the standard deviation of the monthly mean values for each month. (b) The monthly anomalies calculated with respect to the reference average 2001-2019 2016-2019 in the surface layer.

reveals a reduction in flights due to the reduction in global travel during the first phase of the pandemic. As for for with ozone, only months where there are at least 7 days are used to make the monthly average otherwise the month is excluded.

300 The anomalies in Fig. 9 are calculated with respect to the whole length of the CO short reference time-series (2001-2019) and therefore, because of the negative trend, more recent years are all biased low compared with the long term average. The negative trend in springtime over the period 2002-2012 is $-1.91\text{ ppbv yr}^{-1}$ (Petetin et al., 2016b). 2016-2019. In 2020, we can see a drop in CO mixing ratios with the lowest values in the time-series being recorded in February 2020.

Since recent years are more likely to have a negative bias with respect to the long term average (2001-2019), in Fig. 10, the anomalies are calculated with respect to the short section of the time-series (2016-2019) as for Fig. 8. Figure 10 shows the anomalies for March, April and May for 2016-2020. In May, towards the end of the lockdown period, the anomaly was (-27.2 ppbv, -15%) and the 95% confidence limit is outside the range of interannual variability. However, inspection of the time-series (Fig. 9) reveals that the greatest anomaly relative to 2001-2019 2016-2019 was actually apparent in February,

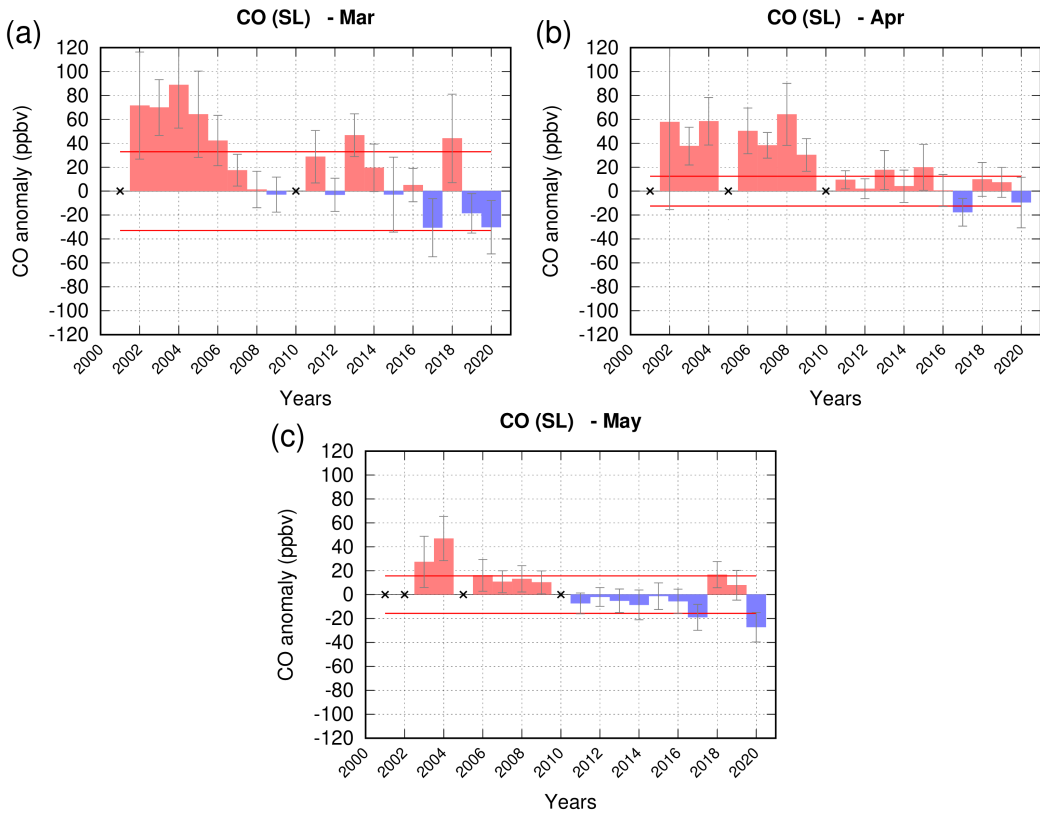


Figure 10. Anomalies of CO for 2016-2020 for all the months of (a) March, (b) April, (c) May, in the surface layer (>950hPa). [The grey bars represent the 95% confidence limits, and the blue horizontal lines represent the interannual variability.](#)

before the European lockdown measures began. When compared with the reference time-series (2016-2019), the anomaly in
 310 February was (-61.4 [ppmv ppbv](#), -26%, see appendix Fig. B1). February lies outside our main period of interest, but the large
 anomaly observed then, suggests that the drop in CO at the surface observed in subsequent months, is not wholly attributed
 to the drop in emissions linked to lockdown. Indeed, a fall in NO₂ levels was also reported by Peuch (2020) from February
 onwards. Peuch (2020) suggested that the driver of this could be an increase in boundary layer heights and consequent dilution
 315 of the pollutants near the surface. To investigate if this could be a factor in the low CO seen in IAGOS data, we examine the
 boundary layer heights for 2020 compared with the 2016-2019 average.

We calculated the boundary layer height (the boundary layer height (BLH) = the boundary layer thickness (zPBL) + orography) by interpolating the ECMWF operational boundary layer heights to the position of the IAGOS aircraft. The ECMWF fields were 1° horizontal resolution and 3 hour time resolution. [We used a bilinear interpolation in space using a distance weighting from the 4 nearest grid cells to the IAGOS position, and a linear interpolation in time.](#) This calculated BLH is one
 320 of a number of added-value products which are included with IAGOS data as a standard in “level 4”. Due to the diurnal variability of the boundary layer height as the convective boundary layer develops during the day, and the seasonal variability in

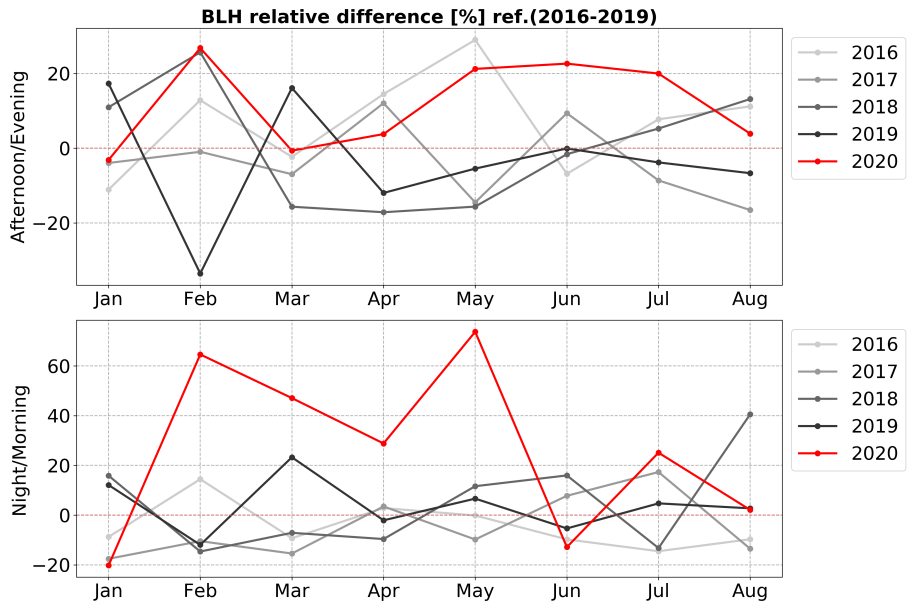


Figure 11. Monthly averaged boundary layer heights interpolated in space and time from the 3hourly ECMWF operational fields on 1°resolution for afternoon/evening (a) and night/morning (b). Afternoon/Evening is defined as 3 hours after sunrise until 2 hours before sunset and Night/morning is defined as 2 hours before sunset until 3 hours after sunrise. The boundary layer heights are expressed as a percentage difference from the mean height calculated over the period 2016-2019.

the time of sunrise and sunset, Fig. 11 is divided into two time slots. The top panel shows the afternoon/evening, defined as 3 hours after sunrise until 2 hours before sunset. The bottom panel shows the nighttime/morning defined as 2 hours before sunset until 3 hours after sunrise. Each time-series shows the percentage difference with respect to the monthly mean calculated for 325 2016-2019 and is shown for 8 months (January-August) for each year between 2016 and 2019. The depth of the nighttime boundary layer increased by 60% (400m) in February and 70% in May with respect to the monthly mean from 2016-2019 and was greater than any other anomaly observed over the period 2016-2019. The anomaly, covers the MAM period and may partly explain the decreased concentrations of CO in the surface layer. We accounted for these changes by integrating the CO over the height of the boundary layer. A negative anomaly of 30ppbv was noted in February and 12ppbv in March and May which can be ascribed to decreases in emissions.

The observations of CO near the surface from IAGOS are less impacted by the local emissions at airports ~~that than~~ might be thought. [Petetin et al \(2018a\)](#) compared IAGOS with monitoring stations from the local Air Quality monitoring network (AQN) and more distant regional surface stations from the Global Atmospheric Watch (GAW) network. They found that the mixing ratios of CO and O₃ close to the surface do not appear to be strongly impacted by local emissions 335 related to airport activities and are not significantly different from those mixing ratios measured at surrounding urban background stations. It is therefore unlikely that the reduction in airport activity during COVID-19 was a big contributor to the

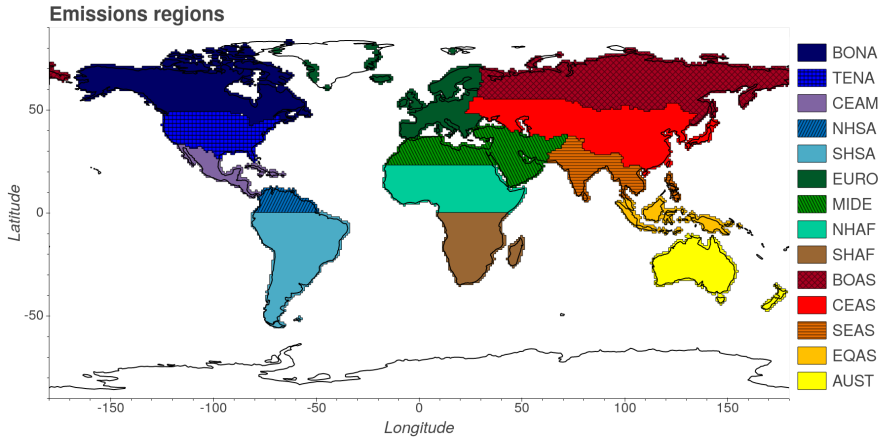


Figure 12. Emissions regions used for the SOFT-IO v1.0 model.

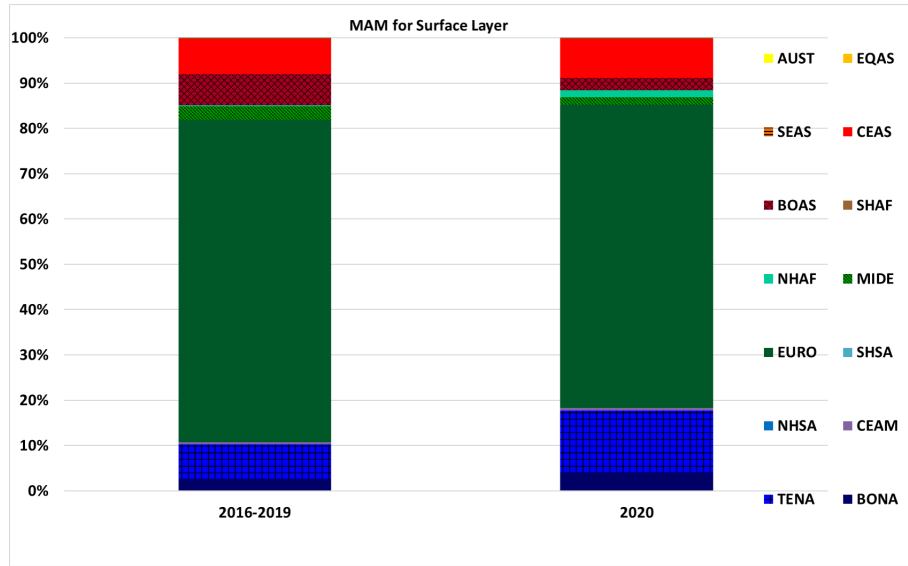


Figure 13. Contribution from different source regions to the CO in the surface layer at Frankfurt in MAM 2020 compared with MAM of 2016-2019. The colours correspond to the regions in Fig. 12.

negative anomaly observed at Frankfurt in the surface layer. In the free troposphere, the local emissions have even less effect and the mixing ratios tend to background concentrations as typically measured by the GAW regional stations.

To examine more closely the source regions of the CO at Frankfurt, we have used the SOFT-IO tool which routinely connects emissions databases to each IAGOS measurement via FLEXPART trajectory calculations (Sauvage et al., 2017b, 2018). 340 **However, due to the SOFT-IO does not calculate the background amounts of CO which include CO from emissions older than 20 days or secondary CO produced by chemical reactions in situ. It is more adapted to look at well-defined plumes of**

345 pollution visible against the background. In addition, the anthropogenic emissions database (MACC-city) ~~not being~~ has not been updated to take account of the COVID-19 period, ~~we will ignore the indicated contribution from fire or anthropogenic sources given by the link to the emissions databases. We present just~~. This make the relative contribution from each source difficult to determine. For these reasons we will focus on the geographic origin of the CO at Frankfurt as determined by the trajectory calculations. The source regions are defined as in Fig. 12. ~~The trajectories terminate at the aircraft position within the surface layer.~~ We compare the source regions in 2020 with those in our reference period 2016-2019. In Fig. 13, we show the source region of the emissions. In agreement with Petetin et al. (2018b), our analysis shows that the largest contribution 350 to CO measured at Frankfurt is from the European region. Usually in this period ~~the~~, the contribution from biomass burning emissions are low, so we deduce that most of the emissions were anthropogenic. In Fig. 13, we show the source region to the surface CO is small. In 2020, there was a smaller absolute contribution to the surface CO from biomass buring emissions (1.3ppbv in 2020 compared with 2.7ppbv in 2016-2019) with the relative contribution being 10% in the reference period. Most 355 of the emissions in Europe in 2020 were therefore anthropogenic. The majority (70%) of the CO at Frankfurt had a European origin in both 2020 and in the reference period of 2016-2019. In 2020, there was a greater contribution from sources in North America (TENA + BONA) and Asia (CEAS) compared with 2016-2019 which reflects the interannual variability of different airmasses arriving in Europe. This analysis shows that it is primarily local emissions across Europe that are reflected in the CO recorded at Frankfurt in the surface layer, and therefore we can suppose that the lockdown measures played a significant role. 360 In the free troposphere, which we discuss in the following section, we ~~shall~~ ~~will~~ see that inter-continental transport has a more important contribution.

2.2.2 Anomalies of Carbon Monoxide in the free troposphere (850-350hPa)

In the free troposphere, the anomalies of CO (Fig. 14) were negative in March (-6.9ppbv, -5%) and May (-1.8 ppbv, ~~4-1%~~) but much smaller in magnitude than in the surface layer (see section 2.2.1) ~~and do not exceed interannual variability once the confidence limits have been considered~~. The time-series of CO in the free troposphere from 2001-2020 is included for 365 reference in Fig. B2. In April, the anomaly was positive (8.2ppbv, 6%). Since the free troposphere is more representative of the background concentrations due to mixing and transport, it is instructive to relate the IAGOS data over Frankfurt to the larger geographical context. Satellite fields of CO in the tropospheric column are presented for Europe in Fig. 15. Figure 15 represents the percentage change in the tropospheric CO at 795 hPa with respect to the 2016-2019 average as retrieved from IASI for the months of March, April, and May. In March, the IASI-SOFRID data confirm the negative anomaly in CO present at Frankfurt, 370 which is generalised over large parts of Europe. In April and May, the IASI-SOFRID data showed little anomaly at Frankfurt and a mixed picture over Europe. Thus, the IAGOS and IASI data show some reduction in CO during the lockdown period which is not unexpected given the trend towards decreased CO. It is difficult to link this anomaly to the lockdown measures due to other factors such as the increased boundary layer height, the long-range global transport of CO, and interannual variability.

375 Using the same trajectory analysis as for Fig. 13, Fig. 16 shows that in MAM 2020, there was a much lower amount of CO from sources in Europe than in MAM 2016-2019, and an increase in the contribution from North America (TENA) and from

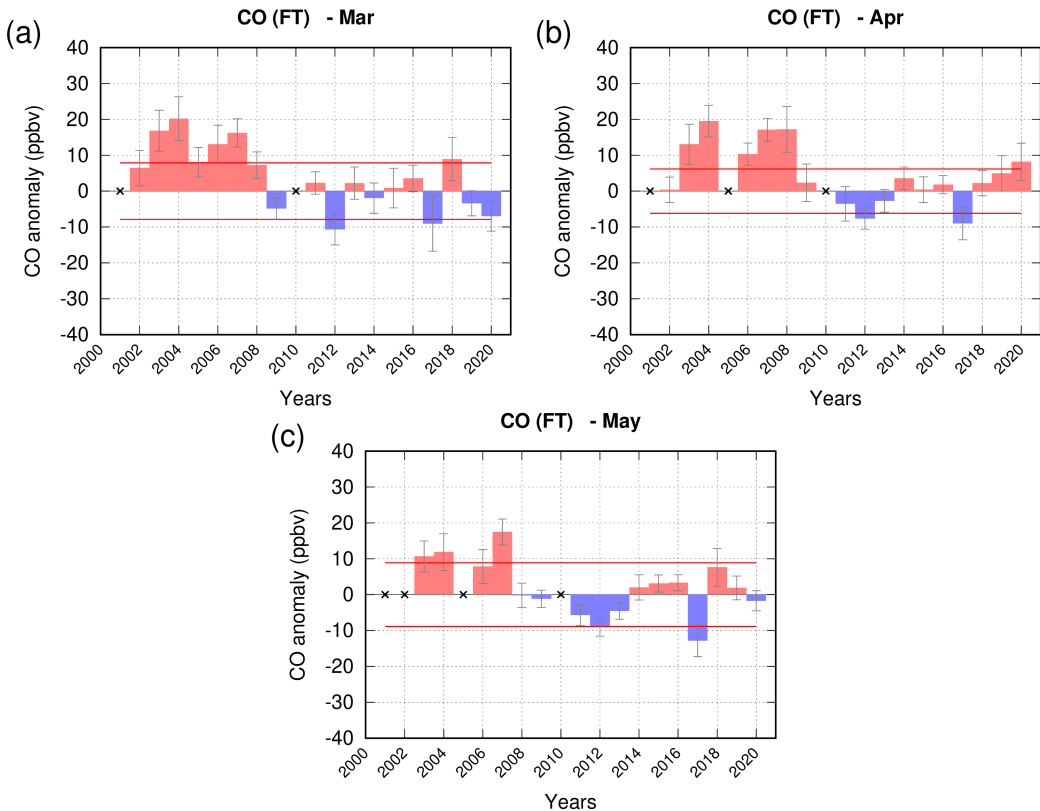


Figure 14. Anomalies of CO for 2016-2020 for all the months of (a) March, (b) April, (c) May, in the free troposphere (850-350hPa). [The grey bars represent the 95% confidence limits, and the blue horizontal lines represent the interannual variability.](#)

Central Asia (CEAS). We suggest that the increase in airmasses [from outside Europe negated carrying CO from anthropogenic and biomass burning sources, from outside Europe off-set](#) the effects of the cut in emissions during the European lockdown resulting in a smaller than anticipated negative anomaly observed by both IAGOS and IASI-SOFRID. This result is similar to 380 that of Field et al. (2020), who noted only a 2% change in background abundances of CO over Eastern China despite the cut in industrial emissions during the Chinese lockdown. In the case of Field et al. (2020) it was the [cross-boundary cross-border](#) transport from areas with active biomass burning that off-set the drop in anthropogenic emissions. [In our reference period, the mean biomass burning contributions were about 3 ppbv or 20%. In 2020, the contribution was 2ppbv. As the contribution from biomass burning is small in Europe in MAM, the main influence to the CO loading over Europe is from anthropogenic](#) 385 [emissions from several source regions with more or less stringent lockdown measures.](#)

In summary for this section on CO, we conclude that the drop in surface CO is largely the result of the drop in emissions during European lockdown, with higher than usual boundary layer heights further diluting the surface concentrations. In the free troposphere, where the negative anomalies were [small not outside expected interannual variability](#), the influence of long range transport is more apparent, and offsets the impact of the reduction in CO emissions across Europe.

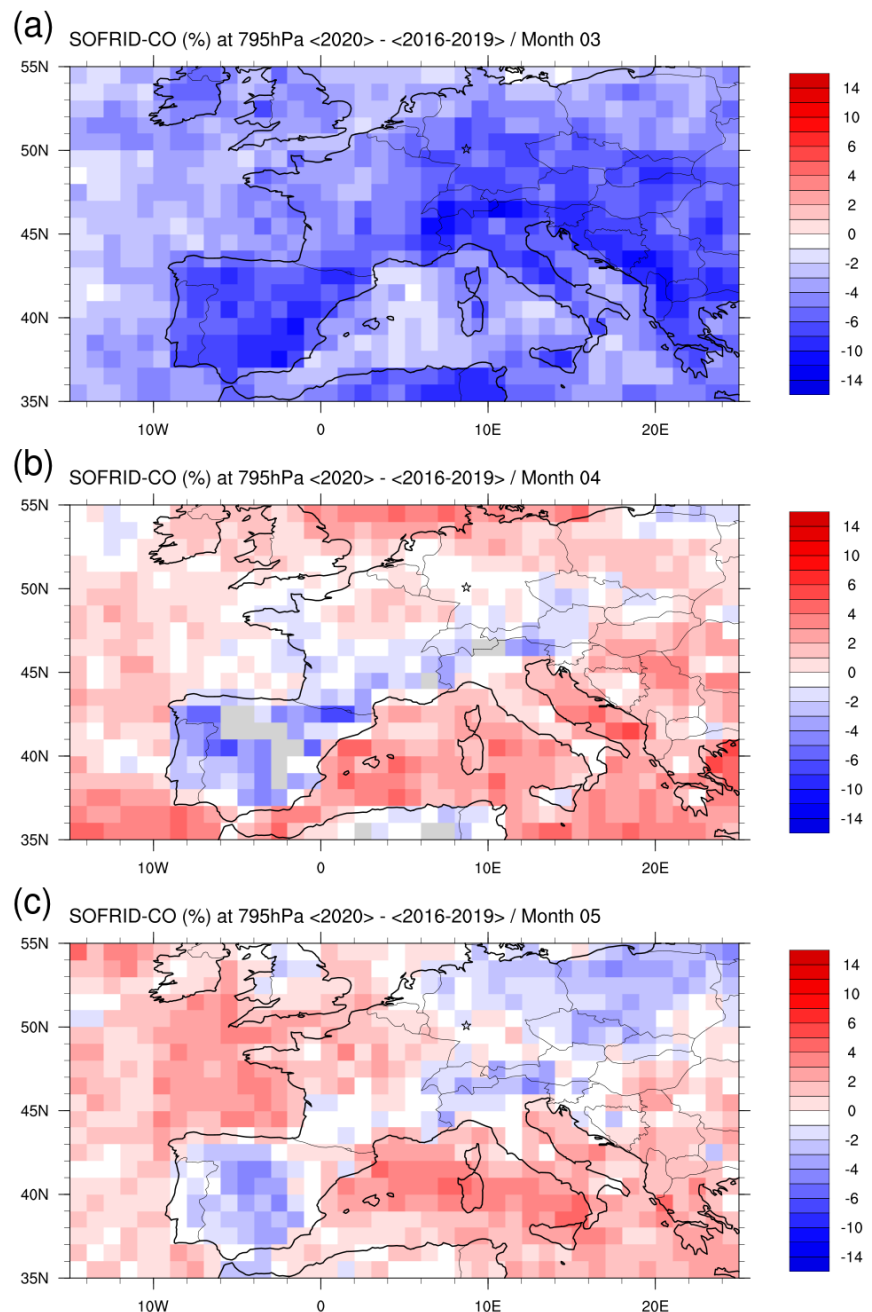


Figure 15. Percentage change of IASI-SOFRID Carbon monoxide at 795hPa in (a) March, (b) April, and (c) May, 2020 compared with the reference average period 2016-2019.

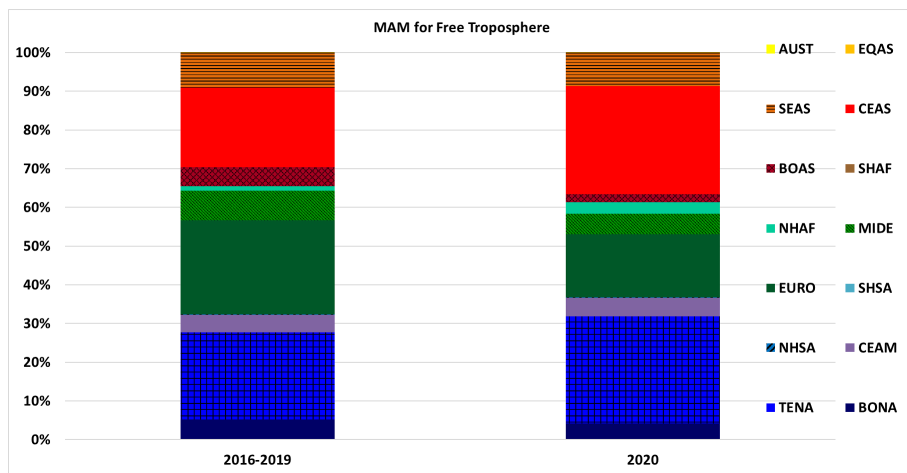


Figure 16. Contribution from different source regions to the CO in the free troposphere at Frankfurt in MAM 2020 compared with MAM of 2016-2019. The colours correspond to the regions in Fig. 12

In this article, we use the IAGOS dataset of in situ observations of ozone and carbon monoxide collected during landing and take-off at Frankfurt airport. The atmosphere is sampled from the surface to the upper troposphere forming a quasi vertical profile. The data form part of a time-series which extends back for 27 years for ozone and 20 years for CO. We considered whether anomalies of ozone and CO at Frankfurt during MAM 2020 were related to changes in atmospheric composition resulting from the COVID-19 lockdowns, which reduced the industrial and traffic emissions of ozone precursors (e.g. Bauwens et al. (2020), Barré et al. (2021)). We compared MAM 2020, with a baseline period of 2016-2019 to account for recent increases in ozone, and decreases in CO. During the springtime (MAM) of 2020, we noted a 2719% increase in ozone in the surface layer (> 950hPa, 600m). The month of May saw the largest anomaly (32%) since the time-series began in 1994. The magnitude of this anomaly is comparable to the European heatwave in August 2003. As this anomaly occurred during the first lockdown period of the COVID-19 outbreak, we thus considered if the anomaly was related to the changes in emissions that resulted from the decreased traffic and industrial activity. The daytime increase

The daytime increase in ozone in May 2020 was significant (19%) but the increase at nighttime (4129%) was double even larger and has not been seen before in the 26 year climatology time-series. Despite the fall in the abundance of NOx over Europe (as seen by satellite data), there were still enough available precursors to produce ozone under the meteorological conditionsthat were very favorable, especially enhanced solar radiation, that prevailed were very favorable at the time (van Heerwaarden et al., 2021). Our The larger increase at nighttime along with the observation that NO₂ fell by between 24% and 33% (Barré et al., 2021), suggests that less ozone was lost through titration with NO due to the reduction in the NO reservoir during the lockdown period, signifying a reduction in the "sink" one of the sinks of ozone. Furthermore, we noted an increase in the depth of the nighttime boundary layer, which would be expected to further reduce the sinks of ozone through less titration and deposition.

The magnitude of this anomaly is comparable to that during the European heatwave in August 2003 which was one of the most significant air-quality events in Europe e.g. Tressol et al. (2008). When compared with the recent reference period 2016-2019, the magnitude of the anomaly in August 2003 is diminished, suggesting that these high ozone abundances are no longer unusual. Although the anomalies of ozone were of similar magnitude to those during the 2003 heatwave, the chemical environment during the lockdown period was quite different. During the 2003 heatwave, IAGOS data showed that there were positive anomalies at Frankfurt in both ozone and the precursor carbon monoxide in the low troposphere (Tressol et al., 2008). The increased CO was due to the transport of plumes from wildfires over Portugal exacerbated by the dry conditions created by the heatwave. Thus, during the 2003 heatwave, the increased ozone was caused the favorable meteorological conditions and an increase in precursors whereas during lockdown, the positive anomaly of ozone was accompanied by favorable meteorology and a fall in precursors.

In the free troposphere, ozone abundances fell slightly. For the period MAM 2020 ozone was 510% lower than the mean 1994-2019 2016-2019 based on the same months. The IAGOS time-series shows that these free tropospheric abundances of ozone were the lowest since 1997 which is probably more reflective of the widespread reduction of emissions over Europe

and beyond, with less impact of local meteorology and chemistry. The results from IAGOS are also consistent with those from
425 the ~~sonde and balloons~~ ~~balloon-borne ozonesondes~~ reported by Steinbrecht et al. (2021) who noted a 7% drop in tropospheric ozone compared with the 2000-2020 climatological mean. They also attributed this to the reduction in pollution during the COVID-19 lockdowns.

A reduction of CO was seen at Frankfurt, with an 11% reduction found in the surface layer but no anomaly in the free troposphere as averaged over MAM. ~~The attribution of this decrease to the drop in emissions during lockdown, is complicated by the fact that the boundary layer heights were anomalously high during this period, and might therefore have contributed to a dilution of the CO at the surface. However, the negative anomalies persist despite controlling for this. It should be noted that the greatest decrease in CO occurred in February, (26%) before lockdown measures had been introduced in Europe. Our trajectory analysis shows that the CO is largely of European origin and therefore we suggest that the anomalies in the surface layer are directly linked to the drop in emissions across Europe due to the lockdown measures. The increase in boundary layer height explains the onset of the anomaly before the onset of lockdown and probably contributed to a further dilution of the CO at the surface~~ ~~the impact of the lockdown on abundances of CO is likely.~~

In the free troposphere there is a small reduction of CO in March (-6.9 ppbv, -5%) and May (~~2 ppbv, 1-1.8 ppbv, -1%~~) which is smaller than at the surface over Frankfurt ~~and remains within the range of interannual variability~~. IASI-SOFRID fields of CO show a clear decrease of CO during March over all of Europe. In April and May small positive and negative anomalies
440 are detected by IASI-SOFRID over northern Europe and mostly negative anomalies over the Iberian Peninsula. In the free troposphere, there is an important role of transport of CO from distant biomass and anthropogenic sources. In particular in MAM 2020, there was a greater contribution from CO originating in North America and Asia ~~which~~ ~~The contribution by airmasses from outside Europe may have~~ off-set some of the ~~drop in CO resulting from the~~ reduction in regional European emissions, with the result that the lockdown measures did not have a big impact on CO in the free ~~tropopshere~~ ~~troposphere~~.

445 The lockdowns provided a unique experiment to assess the impact of a reduction of economic activities on atmospheric composition and climate. The IAGOS data complement other in-situ data from the ozonesonde network, with the added value of having ozone precursors measured simultaneously. This study ~~highlights demonstrates~~ the importance of long and continuous time-series in setting this brief period in context since there are many competing factors and it is difficult to attribute a single cause. We ~~have considered various meteorological factors for both ozone and CO near the surface, and for interannual variability and long range transport in the free troposphere. We~~ look forward to future model sensitivity studies to separate these factors and to provide a more realistic magnitude of the impact of lockdown on the environment.

Data availability. The IAGOS data are available through the IAGOS data portal at <https://doi.org/10.25326/20> (Boulanger, 2020). The IAGOS time series data set used for this analysis is referenced at <https://doi.org/10.25326/06> (Boulanger et al., 2018). The SOFRID-O3 and CO data are freely available on the IASI-SOFRID website (<http://thredds.sedoo.fr/iasi-sofrid-o3-co/>, last access: 31st May 2021; SEDOO, 455 2014).

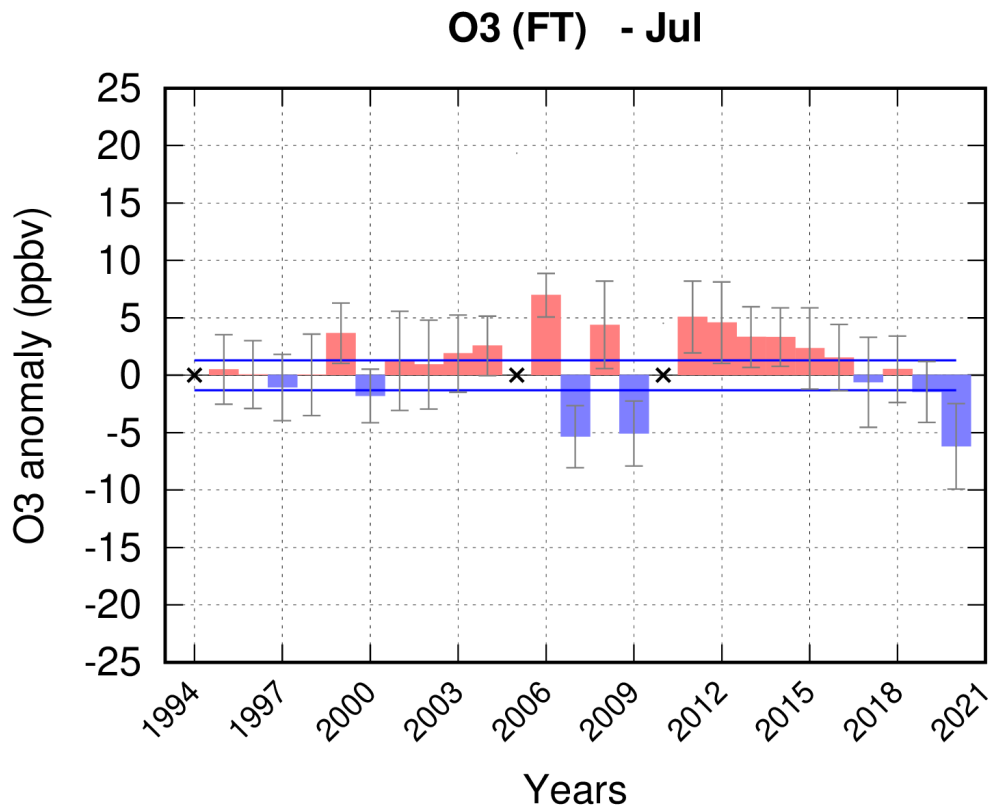


Figure A1. Ozone anomalies in the free troposphere (830-350hPa) for all the months of July since 1994. The grey bars represent the 95% confidence limits, and the blue horizontal lines represent the interannual variability.

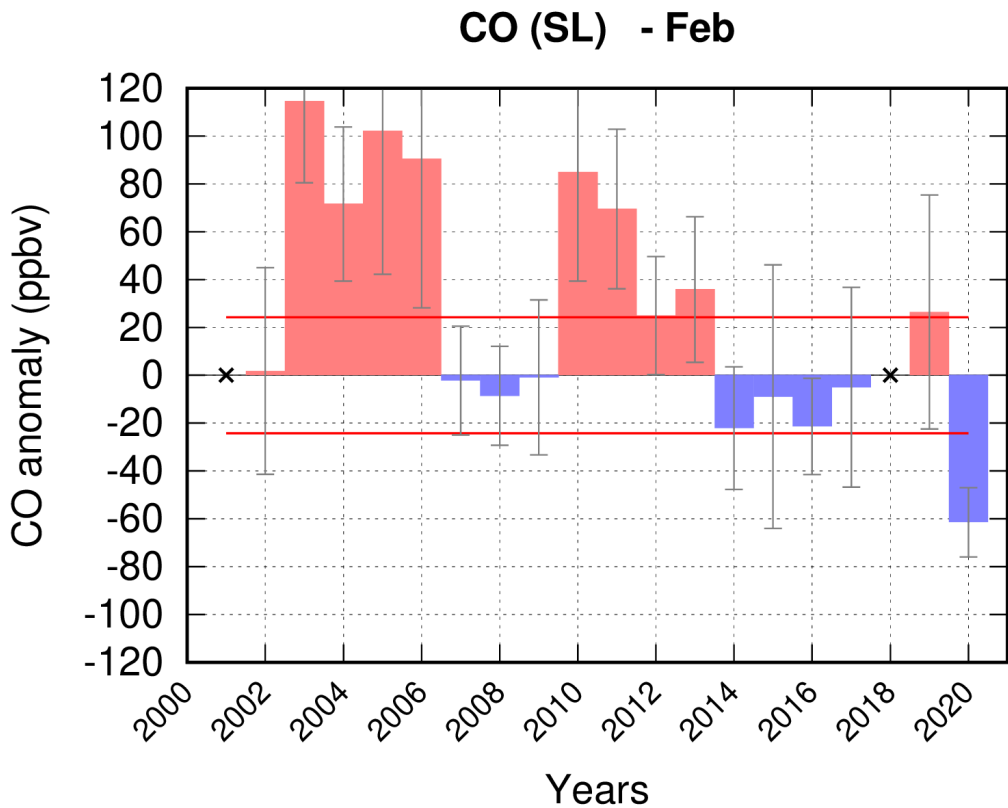


Figure B1. Anomalies of CO from 2016-2019 for all the months of February since 2016 in the surface layer (>950hPa) for all the months of February since 2001. The grey bars represent the 95% confidence limits, and the blue horizontal lines represent the interannual variability.

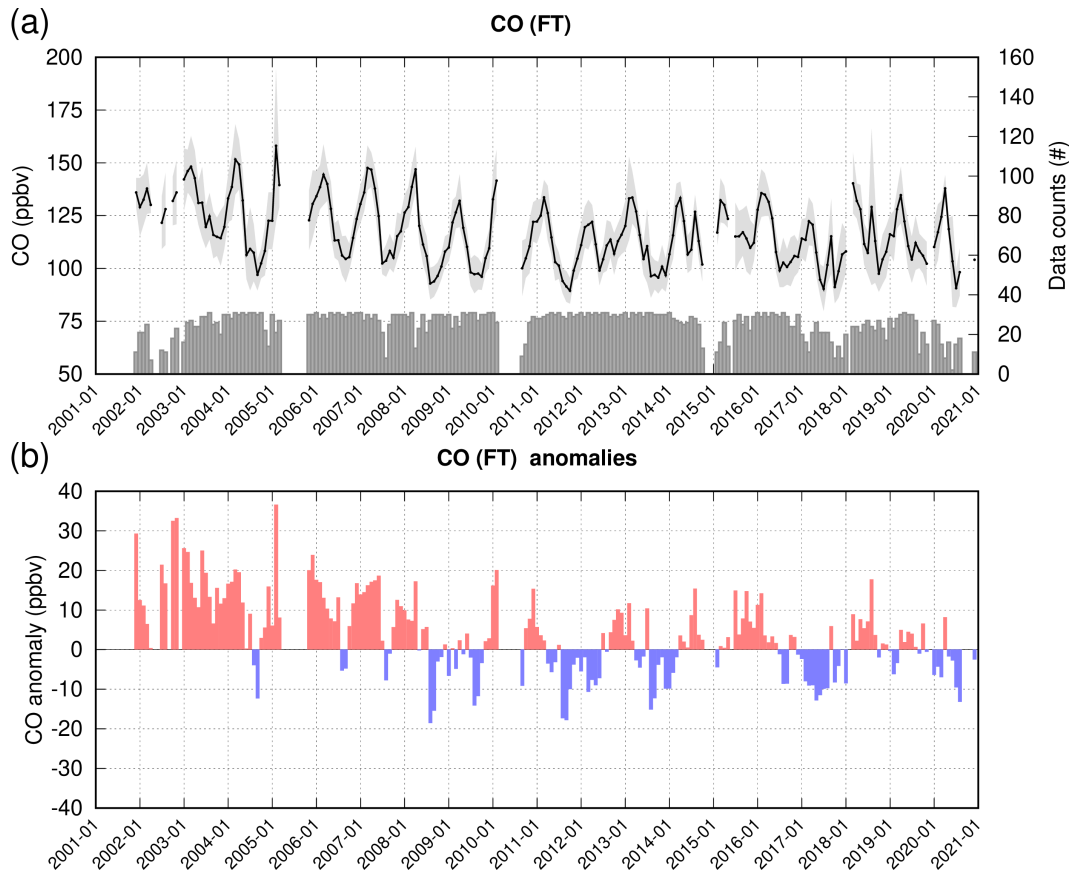


Figure B2. Monthly time-series for 2001–2020 of CO for the free troposphere over Frankfurt (a). The grey bars represent the number of daily profiles used to calculate the monthly means shown in black. Grey shading represents the standard deviation [of the monthly mean values for each month](#). (b) The monthly anomalies calculated with respect to the reference average [2001–2019](#) [2016–2019](#) in the free troposphere (830–350hPa).

Author contributions. HC, YB, and VT designed the study and prepared the paper with contributions from all co-authors. YB developed the code in the framework of the CAMS-84 project. MT, PW, BS are responsible for the level 4 value added products. PhN, RB and JMC produced, validated and calibrated the IAGOS data. DB develops and maintains the IAGOS database. EF and BB performed the IASI-SOFRID retrievals. HC, YB, BS, PhN, VT and AP reviewed and edited.

460 *Competing interests.* The authors declare that they have no conflict of interest.

Acknowledgements. IAGOS has been funded by the European Union projects IAGOS-DS and IAGOS-ERI. The IAGOS database is supported in France by AERIS (<https://www.aeris-data.fr>). We acknowledge the strong support of the European Commission, Airbus and the airlines (Deutsche Lufthansa, Air France, Cathay Pacific, Iberia, China Airlines and Hawaiian Airlines) that carry the IAGOS equipment. In particular we would like to thank Deutsche Lufthansa for operating D-AIKO in a cargo configuration during the COVID-19 period. IASI is a
465 joint mission of EUMETSAT and the Centre National d'Etudes Spatiales (CNES, France). The authors acknowledge the CNES for financial support for the IASI activities and the Bonus Stratégique programme at Université Paul Sabatier Toulouse III who fund Maria Tsivlidou.

References

Akritidis, D., Katragkou, E., Zanis, P., Pytharoulis, I., Melas, D., Flemming, J., Inness, A., Clark, H., Plu, M., and Eskes, H.: A deep stratosphere-to-troposphere ozone transport event over Europe simulated in CAMS global and regional forecast systems: analysis and evaluation, *Atmospheric Chemistry and Physics*, 18, 15 515–15 534, <https://doi.org/10.5194/acp-18-15515-2018>, 2018.

Baldasano, J. M.: COVID-19 lockdown effects on air quality by NO₂ in the cities of Barcelona and Madrid (Spain), *Science of The Total Environment*, 741, 140 353, <https://doi.org/https://doi.org/10.1016/j.scitotenv.2020.140353>, 2020.

Barré, J., Petetin, H., Colette, A., Guevara, M., Peuch, V.-H., Rouil, L., Engelen, R., Inness, A., Flemming, J., Pérez García-Pando, C., Bowdalo, D., Meleux, F., Geels, C., Christensen, J. H., Gauss, M., Benedictow, A., Tsyro, S., Friese, E., Struzewska, J., Kaminski, J. W., Douros, J., Timmermans, R., Robertson, L., Adani, M., Jorba, O., Joly, M., and Kouznetsov, R.: Estimating lockdown-induced European NO₂ changes using satellite and surface observations and air quality models, *Atmospheric Chemistry and Physics*, 21, 7373–7394, <https://doi.org/10.5194/acp-21-7373-2021>, 2021.

Barret, B., Le Flochmoen, E., Sauvage, B., Pavelin, E., Matricardi, M., and Cammas, J. P.: The detection of post-monsoon tropospheric ozone variability over south Asia using IASI data, *Atmospheric Chemistry and Physics*, 11, 9533–9548, <https://doi.org/10.5194/acp-11-9533-2011>, 2011.

Bauwens, M., Compernolle, S., Stavrakou, T., Müller, J.-F., van Gent, J., Eskes, H., Levelt, P. F., van der A, R., Veefkind, J. P., Vlietinck, J., Yu, H., and Zehner, C.: Impact of Coronavirus Outbreak on NO₂ Pollution Assessed Using TROPOMI and OMI Observations, *Geophysical Research Letters*, 47, e2020GL087978, <https://doi.org/https://doi.org/10.1029/2020GL087978>, e2020GL087978 2020GL087978, 2020.

Beirle, S., Platt, U., Wenig, M., and Wagner, T.: Weekly cycle of NO₂ by GOME measurements: a signature of anthropogenic sources, *Atmospheric Chemistry and Physics*, 3, 2225–2232, <https://doi.org/10.5194/acp-3-2225-2003>, 2003.

Blot, R., Nedelec, P., Boulanger, D., Wolff, P., Sauvage, B., Cousin, J.-M., Athier, G., Zahn, A., Obersteiner, F., Scharffe, D., Petetin, H., Bennouna, Y., Clark, H., and Thouret, V.: Internal consistency of the IAGOS ozone and carbon monoxide measurements for the last 25 years, *Atmospheric Measurement Techniques*, 14, 3935–3951, <https://doi.org/10.5194/amt-14-3935-2021>, 2021.

Clerbaux, C., Boynard, A., Clarisse, L., George, M., Hadji-Lazaro, J., Herbin, H., Hurtmans, D., Pommier, M., Razavi, A., Turquety, S., Wespes, C., and Coheur, P.-F.: Monitoring of atmospheric composition using the thermal infrared IASI/MetOp sounder, *Atmospheric Chemistry and Physics*, 9, 6041–6054, <https://doi.org/10.5194/acp-9-6041-2009>, 2009.

Cooper, O. R., Schultz, M. G., Schröder, S., Chang, K.-L., Gaudel, A., Benítez, G. C., Cuevas, E., Fröhlich, M., Galbally, I. E., Molloy, S., Kubistin, D., Lu, X., McClure-Begley, A., Nédélec, P., O'Brien, J., Oltmans, S. J., Petropavlovskikh, I., Ries, L., Senik, I., Sjöberg, K., Solberg, S., Spain, G. T., Spangl, W., Steinbacher, M., Tarasick, D., Thouret, V., and Xu, X.: Multi-decadal surface ozone trends at globally distributed remote locations, *Elementa: Science of the Anthropocene*, 8, <https://doi.org/10.1525/elementa.420>, 23, 2020.

De Wachter, E., Barret, B., Le Flochmoën, E., Pavelin, E., Matricardi, M., Clerbaux, C., Hadji-Lazaro, J., George, M., Hurtmans, D., Coheur, P.-F., Nédélec, P., and Cammas, J. P.: Retrieval of MetOp-A/IASI CO profiles and validation with MOZAIC data, *Atmospheric Measurement Techniques*, 5, 2843–2857, <https://doi.org/10.5194/amt-5-2843-2012>, 2012.

Field, R. D., Hickman, J. E., Geogdzhayev, I. V., Tsigaridis, K., and Bauer, S. E.: Changes in satellite retrievals of atmospheric composition over eastern China during the 2020 COVID-19 lockdowns, *Atmospheric Chemistry and Physics Discussions*, 2020, 1–31, <https://doi.org/10.5194/acp-2020-567>, 2020.

Forster, C., Stohl, A., and Seibert, P.: Parameterization of Convective Transport in a Lagrangian Particle Dispersion Model and Its Evaluation, *Journal of Applied Meteorology and Climatology*, 46, 403 – 422, <https://doi.org/10.1175/JAM2470.1>, 2007.

505 Gaudel, A., Cooper, O. R., Chang, K.-L., Bourgeois, I., Ziemke, J. R., Strode, S. A., Oman, L. D., Sellitto, P., Nédélec, P., Blot, R., Thouret, V., and Granier, C.: Aircraft observations since the 1990s reveal increases of tropospheric ozone at multiple locations across the Northern Hemisphere, *Science Advances*, 6, <https://doi.org/10.1126/sciadv.aba8272>, 2020.

Gettelman, A., Hoor, P. P., Pan, L. L., Randel, W. J., Hegglin, M. I., and Birner, T.: The Extratropical Upper Troposphere and Lower Stratosphere, *Reviews of Geophysics*, 49, [https://doi.org/https://doi.org/10.1029/2011RG000355](https://doi.org/10.1029/2011RG000355), 2011.

510 Gkatzelis, G. I., Gilman, J. B., Brown, S. S., Eskes, H., Gomes, A. R., Lange, A. C., McDonald, B. C., Peischl, J., Petzold, A., Thompson, C. R., and Kiendler-Scharr, A.: The global impacts of COVID-19 lockdowns on urban air pollution: A critical review and recommendations, *Elementa: Science of the Anthropocene*, 9, <https://doi.org/10.1525/elementa.2021.00176>, 00176, 2021.

515 Goldberg, D. L., Anenberg, S. C., Griffin, D., McLinden, C. A., Lu, Z., and Streets, D. G.: Disentangling the Impact of the COVID-19 Lockdowns on Urban NO₂ From Natural Variability, *Geophysical Research Letters*, 47, e2020GL089269, <https://doi.org/https://doi.org/10.1029/2020GL089269>, 2020.

Grange, S. K., Lee, J. D., Drysdale, W. S., Lewis, A. C., Hueglin, C., Emmenegger, L., and Carslaw, D. C.: COVID-19 lockdowns highlight a risk of increasing ozone pollution in European urban areas, *Atmospheric Chemistry and Physics*, 21, 4169–4185, <https://doi.org/10.5194/acp-21-4169-2021>, 2021.

520 Holton, J. R., Haynes, P. H., McIntyre, M. E., Douglass, A. R., Rood, R. B., and Pfister, L.: Stratosphere-troposphere exchange, *Reviews of Geophysics*, 33, 403–439, <https://doi.org/https://doi.org/10.1029/95RG02097>, 1995.

Le Quéré, C., Jackson, R., Jones, M., Smith, A., Abernethy, S., Andrew, R., De-Gol, A., Willis, D., Shan, Y., Canadell, J., Friedlingstein, P., Creutzig, F., and Peters, G.: Temporary reduction in daily global CO₂ emissions during the COVID-19 forced confinement, *Nature Climate Change*, 10, 1–7, <https://doi.org/10.1038/s41558-020-0797-x>, 2020.

525 Lee, J. D., Drysdale, W. S., Finch, D. P., Wilde, S. E., and Palmer, P. I.: UK surface NO₂ levels dropped by 42 % during the COVID-19 lockdown: impact on surface O₃, *Atmospheric Chemistry and Physics*, 20, 15 743–15 759, <https://doi.org/10.5194/acp-20-15743-2020>, 2020.

Liu, F., Page, A., Strode, S. A., Yoshida, Y., Choi, S., Zheng, B., Lamsal, L. N., Li, C., Krotkov, N. A., Eskes, H., van der A, R., Veefkind, P., Levelt, P. F., Hauser, O. P., and Joiner, J.: Abrupt decline in tropospheric nitrogen dioxide over China after the outbreak of COVID-19, *Science Advances*, 6, eabc2992, <https://doi.org/10.1126/sciadv.abc2992>, 2020.

530 Marenco, A., Thouret, V., Nédélec, P., Smit, H., Helten, M., Kley, D., Karcher, F., Simon, P., Law, K., Pyle, J., Poschmann, G., Von Wrede, R., Hume, C., and Cook, T.: Measurement of ozone and water vapor by Airbus in-service aircraft: The MOZAIC airborne program, an overview, *Journal of Geophysical Research: Atmospheres*, 103, 25 631–25 642, <https://doi.org/https://doi.org/10.1029/98JD00977>, 1998.

Matricardi, M., Chevallier, F., Kelly, G., and Thépaut, J.-N.: An improved general fast radiative transfer model for the assimilation of radiance observations, *Quarterly Journal of the Royal Meteorological Society*, 130, 153–173, <https://doi.org/https://doi.org/10.1256/qj.02.181>, 2004.

535 Monks, P. S.: Gas-phase radical chemistry in the troposphere, *Chem. Soc. Rev.*, 34, 376–395, <https://doi.org/10.1039/B307982C>, 2005.

Nédélec, P., Cammas, J.-P., Thouret, V., Athier, G., Cousin, J.-M., Legrand, C., Abonnel, C., Lecoeur, F., Cayez, G., and Marizy, C.: An improved infrared carbon monoxide analyser for routine measurements aboard commercial airbus aircraft: Technical validation and first scientific results of the MOZAIC III programme, *Atmospheric Chemistry and Physics Discussions*, 3, 3713–3744, <https://hal.archives-ouvertes.fr/hal-00327862>, 2003.

Nédélec, P., Blot, R., Boulanger, D., Athier, G., Cousin, J.-M., Gautron, B., Petzold, A., Volz-Thomas, A., and Thouret, V.: Instrumentation on commercial aircraft for monitoring the atmospheric composition on a global scale: the IAGOS system, technical overview of ozone and carbon monoxide measurements, *Tellus B: Chemical and Physical Meteorology*, 67, 27 791, <https://doi.org/10.3402/tellusb.v67.27791>, 2015.

545 Ordóñez, C., Garrido-Perez, J. M., and García-Herrera, R.: Early spring near-surface ozone in Europe during the COVID-19 shutdown: Meteorological effects outweigh emission changes, *Science of The Total Environment*, 747, 141 322, <https://doi.org/https://doi.org/10.1016/j.scitotenv.2020.141322>, 2020.

Ordóñez, C., Elguindi, N., Stein, O., Huijnen, V., Flemming, J., Inness, A., Flentje, H., Katragkou, E., Moinat, P., Peuch, V.-H., Segers, A., Thouret, V., Athier, G., van Weele, M., Zerefos, C. S., Cammas, J.-P., and Schultz, M. G.: Global model simulations of air pollution during 550 the 2003 European heat wave, *Atmospheric Chemistry and Physics*, 10, 789–815, <https://doi.org/10.5194/acp-10-789-2010>, 2010.

Pathakoti, M., Muppalla, A., Hazra, S., D. Venkata, M., A. Lakshmi, K., K. Sagar, V., Shekhar, R., Jella, S., M. V. Rama, S. S., and Vijayasundaram, U.: Measurement report: An assessment of the impact of a nationwide lockdown on air pollution – a remote sensing perspective over India, *Atmospheric Chemistry and Physics Discussions*, 2021, 1–30, <https://doi.org/10.5194/acp-2020-1227>, 2021.

Pavelin, E. G., English, S. J., and Eyre, J. R.: The assimilation of cloud-affected infrared satellite radiances for numerical weather prediction, 555 *Quarterly Journal of the Royal Meteorological Society*, 134, 737–749, <https://doi.org/https://doi.org/10.1002/qj.243>, 2008.

Petetin, H., Thouret, V., Athier, G., Blot, R., Boulanger, D., Cousin, J.-M., Gaudel, A., Nédélec, P., and Cooper, O.: Diurnal cycle of ozone throughout the troposphere over Frankfurt as measured by MOZAIC-IAGOS commercial aircraft, *Elementa: Science of the Anthropocene*, 4, <https://doi.org/10.12952/journal.elementa.000129>, 000129, 2016a.

Petetin, H., Thouret, V., Fontaine, A., Sauvage, B., Athier, G., Blot, R., Boulanger, D., Cousin, J.-M., and Nédélec, P.: Characterising 560 tropospheric O₃ and CO around Frankfurt over the period 1994–2012 based on MOZAIC–IAGOS aircraft measurements, *Atmospheric Chemistry and Physics*, 16, 15 147–15 163, <https://doi.org/10.5194/acp-16-15147-2016>, 2016b.

Petetin, H., Jeoffrion, M., Sauvage, B., Athier, G., Blot, R., Boulanger, D., Clark, H., Cousin, J.-M., Gheusi, F., Nédélec, P., Steinbacher, M., and Thouret, V.: Representativeness of the IAGOS airborne measurements in the lower troposphere, *Elementa: Science of the Anthropocene*, 6, <https://doi.org/10.1525/elementa.280>, 23, 2018a.

565 Petetin, H., Sauvage, B., Parrington, M., Clark, H., Fontaine, A., Athier, G., Blot, R., Boulanger, D., Cousin, J.-M., Nédélec, P., and Thouret, V.: The role of biomass burning as derived from the tropospheric CO vertical profiles measured by IAGOS aircraft in 2002–2017, *Atmospheric Chemistry and Physics*, 18, 17 277–17 306, <https://doi.org/10.5194/acp-18-17277-2018>, 2018b.

Petetin, H., Bowdalo, D., Soret, A., Guevara, M., Jorba, O., Serradell, K., and Pérez García-Pando, C.: Meteorology-normalized impact of the 570 COVID-19 lockdown upon NO₂ pollution in Spain, *Atmospheric Chemistry and Physics*, 20, 11 119–11 141, <https://doi.org/10.5194/acp-20-11119-2020>, 2020.

Petzold, A., Thouret, V., Gerbig, C., Zahn, A., Brenninkmeijer, C. A. M., Gallagher, M., Hermann, M., Pontaud, M., Ziereis, H., Boulanger, D., Marshall, J., Nédélec, P., Smit, H. G. J., Friess, U., Flaud, J.-M., Wahner, A., Cammas, J.-P., Volz-Thomas, A., and TEAM, I.: Global-scale atmosphere monitoring by in-service aircraft – current achievements and future prospects of the European Research Infrastructure IAGOS, *Tellus B: Chemical and Physical Meteorology*, 67, 28 452, <https://doi.org/10.3402/tellusb.v67.28452>, 2015.

575 Peuch, V.-H.: CAMS contribution to the study of air pollution links to COVID-19, pp. 20–23, <https://doi.org/10.21957/j83phv41ok>, 2020.

Saunders, R., Matricardi, M., and Brunel, P.: An improved fast radiative transfer model for assimilation of satellite radiance observations, *Quarterly Journal of the Royal Meteorological Society*, 125, 1407–1425, <https://doi.org/https://doi.org/10.1002/qj.1999.49712555615>, 1999.

Sauvage, B., Auby, A., and Fontaine, A.: Source attribution using FLEXPART and carbon monoxide emission inventories: SOFT-IO version 580 1.0, <https://doi.org/10.25326/2>, 2017a.

Sauvage, B., Fontaine, A., Eckhardt, S., Auby, A., Boulanger, D., Petetin, H., Paugam, R., Athier, G., Cousin, J.-M., Darras, S., Nédélec, P., Stohl, A., Turquety, S., Cammas, J.-P., and Thouret, V.: Source attribution using FLEXPART and carbon monoxide emission inventories: SOFT-IO version 1.0, *Atmospheric Chemistry and Physics*, 17, 15 271–15 292, <https://doi.org/10.5194/acp-17-15271-2017>, 2017b.

Sauvage, B., Nédélec, P., and Boulanger, D.: IAGOS ancillary data (L4) - CO contributions to the aircraft measurements, 585 <https://doi.org/10.25326/3>, 2018.

Schiermeier, Q.: Why pollution is plummeting in some cities — but not others, *Nature*, 580, <https://doi.org/10.1038/d41586-020-01049-6>, 2020.

Schumann, U., Bugliaro, L., Dörnbrack, A., Baumann, R., and Voigt, C.: Aviation Contrail Cirrus and Radiative Forcing Over Europe During 590 6 Months of COVID-19, *Geophysical Research Letters*, 48, e2021GL092 771, <https://doi.org/https://doi.org/10.1029/2021GL092771>, e2021GL092771 2021GL092771, 2021a.

Schumann, U., Poll, I., Teoh, R., Koelle, R., Spinielli, E., Molloy, J., Koudis, G. S., Baumann, R., Bugliaro, L., Stettler, M., and Voigt, C.: Air traffic and contrail changes during COVID-19 over Europe: A model study, *Atmospheric Chemistry and Physics Discussions*, 2021, 1–37, <https://doi.org/10.5194/acp-2021-62>, 2021b.

Shi, X. and Brasseur, G. P.: The Response in Air Quality to the Reduction of Chinese Economic Activities During the COVID-19 595 Outbreak, *Geophysical Research Letters*, 47, e2020GL088 070, <https://doi.org/https://doi.org/10.1029/2020GL088070>, e2020GL088070 2020GL088070, 2020.

Sicard, P., De Marco, A., Agathokleous, E., Feng, Z., Xu, X., Paoletti, E., Rodriguez, J. J. D., and Calatayud, V.: Amplified ozone pollution in cities during the COVID-19 lockdown, *Science of The Total Environment*, 735, 139 542, <https://doi.org/https://doi.org/10.1016/j.scitotenv.2020.139542>, 2020.

Steinbrecht, W., Kubistin, D., Plass-Dülmer, C., Davies, J., Tarasick, D. W., Gathen, P. v. d., Deckelmann, H., Jepsen, N., Kivi, R., Lyall, 600 N., Palm, M., Notholt, J., Kois, B., Oelsner, P., Allaart, M., Piters, A., Gill, M., Van Malderen, R., Delcloo, A. W., Sussmann, R., Mahieu, E., Servais, C., Romanens, G., Stübi, R., Ancellet, G., Godin-Beekmann, S., Yamanouchi, S., Strong, K., Johnson, B., Cullis, P., Petropavlovskikh, I., Hannigan, J. W., Hernandez, J.-L., Diaz Rodriguez, A., Nakano, T., Chouza, F., Leblanc, T., Torres, C., Garcia, O., Röhling, A. N., Schneider, M., Blumenstock, T., Tully, M., Paton-Walsh, C., Jones, N., Querel, R., Strahan, S., Stauffer, R. M., Thompson, A. M., Inness, A., Engelen, R., Chang, K.-L., and Cooper, O. R.: COVID-19 Crisis Reduces Free Tropospheric Ozone Across the Northern Hemisphere, *Geophysical Research Letters*, 48, e2020GL091 987, <https://doi.org/https://doi.org/10.1029/2020GL091987>, e2020GL091987 2020GL091987, 2021.

Stohl, A., Forster, C., Frank, A., Seibert, P., and Wotawa, G.: Technical note: The Lagrangian particle dispersion model FLEXPART version 6.2, *Atmospheric Chemistry and Physics*, 5, 2461–2474, <https://doi.org/10.5194/acp-5-2461-2005>, 2005.

Tan, P.-H., Chou, C., Liang, J.-Y., Chou, C. C.-K., and Shiu, C.-J.: Air pollution “holiday effect” resulting from the Chinese New Year, 610 *Atmospheric Environment*, 43, 2114–2124, <https://doi.org/https://doi.org/10.1016/j.atmosenv.2009.01.037>, 2009.

Thouret, V., Marenco, A., Logan, J. A., Nédélec, P., and Grouhel, C.: Comparisons of ozone measurements from the MOZAIC airborne program and the ozone sounding network at eight locations, *Journal of Geophysical Research: Atmospheres*, 103, 25 695–25 720, <https://doi.org/https://doi.org/10.1029/98JD02243>, 1998.

615 Tressol, M., Ordonez, C., Zbinden, R., Brioude, J., Thouret, V., Mari, C., Nédélec, P., Cammas, J.-P., Smit, H., Patz, H.-W., and Volz-Thomas, A.: Air pollution during the 2003 European heat wave as seen by MOZAIC airliners, *Atmospheric Chemistry and Physics*, 8, 2133–2150, <https://doi.org/10.5194/acp-8-2133-2008>, 2008.

620 van Heerwaarden, C. C., Mol, W. B., Veerman, M. A., Benedict, I., Heusinkveld, B. G., Knap, W. H., Kazadzis, S., Kouremeti, N., and Fiedler, S.: Record high solar irradiance in Western Europe during first COVID-19 lockdown largely due to unusual weather, *Communications Earth and Environment*, 2, 37, <https://doi.org/10.1038/s43247-021-00110-0>, 2021.

625 Veefkind, J., Aben, I., McMullan, K., Förster, H., de Vries, J., Otter, G., Claas, J., Eskes, H., de Haan, J., Kleipool, Q., van Weele, M., Hasekamp, O., Hoogeveen, R., Landgraf, J., Snel, R., Tol, P., Ingmann, P., Voors, R., Kruizinga, B., Vink, R., Visser, H., and Levelt, P.: TROPOMI on the ESA Sentinel-5 Precursor: A GMES mission for global observations of the atmospheric composition for climate, air quality and ozone layer applications, *Remote Sensing of Environment*, 120, 70–83, <https://doi.org/https://doi.org/10.1016/j.rse.2011.09.027>, the Sentinel Missions - New Opportunities for Science, 2012.

630 Wang, W., Parrish, D. D., Li, X., Shao, M., Liu, Y., Mo, Z., Lu, S., Hu, M., Fang, X., Wu, Y., Zeng, L., and Zhang, Y.: Exploring the drivers of the increased ozone production in Beijing in summertime during 2005–2016, *Atmospheric Chemistry and Physics*, 20, 15 617–15 633, <https://doi.org/10.5194/acp-20-15617-2020>, 2020a.

Wang, Y., Yuan, Y., Wang, Q., Liu, C., Zhi, Q., and Cao, J.: Changes in air quality related to the control of coronavirus in China: Implications for traffic and industrial emissions, *Science of The Total Environment*, 731, 139 133, <https://doi.org/https://doi.org/10.1016/j.scitotenv.2020.139133>, 2020b.

WHO: World Health Organisation, Coronavirus disease (COVID-19) pandemic, <https://www.euro.who.int/en/health-topics/health-emergencies/coronavirus-covid-19/novel-coronavirus-2019-ncov>, last accessed: 09/12/2020, 2020.